AD-A141 021 ANALYTICAL AND EXPERIMENTAL STUDY OF GROOVED PAVEMENT RUNOFF(U) PENNSYLVANIA TRANSPORTATION INST UNIVERSITY PARK J R REED ET AL. AUG 83 PTI-8318 DOT/FAA/PM-83/34 1/1

UNCLASSIFIED DTFA01-81-C-10037 F/G 1/5 NL

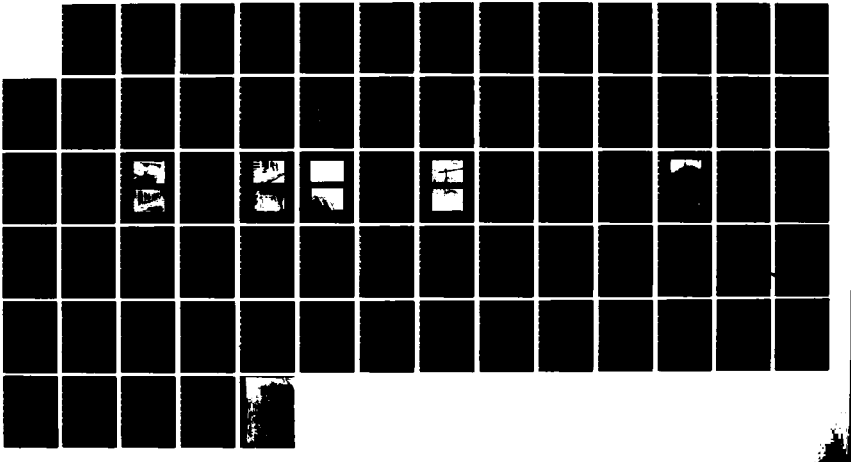

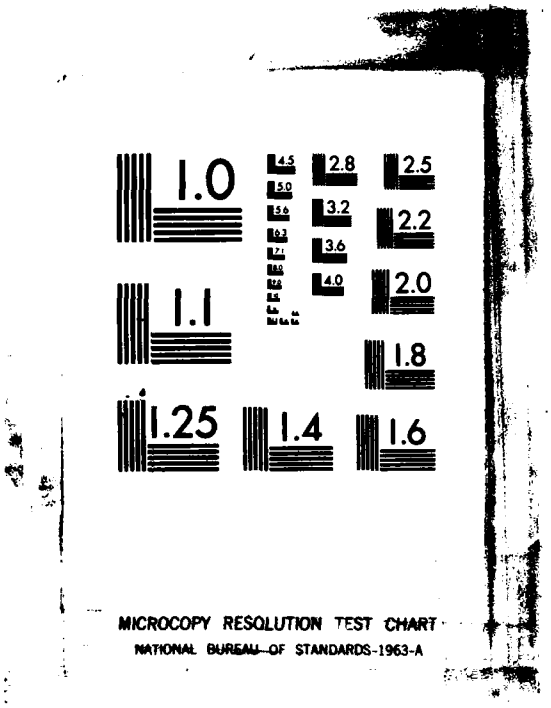
1.0
1.1
1.25
1.4
1.6
2.0
2.2
2.5
2.8
3.2
3.6
4.0
4.5
5.0
5.6
6.3
7.1
8.0
MICROCOPY RESOLUTION TEST CHART
NATIONAL BUREAU OF STANDARDS-1963-A

(13)

DOT/FAA/PM-83/34

Program Engineering &
Maintenance Service
Washington, D.C. 20591

# Analytical and Experimental Study of Grooved Pavement Runoff

J.R. Reed
D.F. Kibler
M.L. Proctor

August 1983



US Department of Transportation
Federal Aviation Administration

## NOTICE

This document is disseminated under the sponsorship of the Department of Transportation in the interest of information exchange. The United States Government assumes no liability for its contents or use thereof.

TECHNICAL REPORT STANDARD TITLE PAGE

| 1. Report No. | 2. Government Accession No. | 3. Recipient's Catalog No. |
|---|---|---|
| DOT/FAA/PM-83/34 | AD-A141 021 | |

| 4. Title and Subtitle | 5. Report Date |
|---|---|
| ANALYTICAL AND EXPERIMENTAL STUDY OF GROOVED PAVEMENT RUNOFF | August 1983 |
| | 6. Performing Organization Code |

| 7. Author(s) | 8. Performing Organization Report No. |
|---|---|
| J. R. Reed, D. F. Kibler, and M. L. Proctor | PTI 8318 |

| 9. Performing Organization Name and Address | 10. Work Unit No. |
|---|---|
| The Pennsylvania Transportation Institute<br>The Pennsylvania State University<br>Research Bldg. B<br>University Park, PA 16802 | 11. Contract or Grant No.<br>DTFA01-81-C-10037 |
| 12. Sponsoring Agency Name and Address | 13. Type of Report and Period Covered |
| U.S. Department of Transportation<br>Federal Aviation Administration<br>Program Engineering & Maintenance Service<br>Washington, D.C. 20591 | Final Report<br>May 1981-August 1983 |
| | 14. Sponsoring Agency Code<br>APM-740 |

15. Supplementary Notes

Progress of this contract was monitored by Mr. Herman D'Aulerio and Dr. Satish K. Agrawal of the Federal Aviation Administration.

16. Abstract

Drainage characteristics of grooved runways were investigated. An analytical model, developed from unsteady flow theory, was solved on a computer in order to predict runoff depths for various rainfall rates on a 100-ft-wide runway sloping transversely at 1.5%. The hydraulic roughness used by the model was predicted from pavement macrotexture. Experiments to check the validity of the model were conducted using artificial rain indoors on a 30-ft-by-15-ft portland cement concrete slab sloping at 1.5% along the 30-ft side. Rainfall rates of 1.15 and 2.45 in./hr were applied to the slab with rectangular grooves parallel to the 30-ft side and spaced at ∞, 5, 2.5, and 1.25 in. Data on the slab surface showed that water depths were smaller, and the hydraulic roughness was larger, than expected. The model was adjusted accordingly, and used to generate curves of water depths and their reductions versus distance out to 100 ft for a rainfall of 3 in./hr and a hydraulic roughness of 0.056. Predicted reductions in water depths ranged from 100% through 39 ft to 27% at 100 ft for the 1.25-in. spacing; from 100% through 19 ft to 14% at 100 ft for the 2.5-in. spacing; and from 100% through 9 ft to 7% at 100 ft for the 5-in. spacing.

| 17. Key Words | 18. Distribution Statement |
|---|---|
| airport runways, grooved pavements, runoff characteristics, drainage, rainfall simulation, hydraulic roughness, pavement texture | Available to the public from:<br>National Technical Information Service<br>U.S. Department of Commerce<br>Springfield, VA 22161. |

| 19. Security Classif. (of this report) | 20. Security Classif. (of this page) | 21. No. of Pages | 22. Price |
|---|---|---|---|
| UNCLASSIFIED | UNCLASSIFIED | 69 | |

Form DOT F 1700.7 (8-69)

## METRIC CONVERSION FACTORS

### Approximate Conversions to Metric Measures

| Symbol | When You Know | Multiply by | To Find | Symbol |
|---|---|---|---|---|
| | **LENGTH** | | | |
| in | inches | *2.5 | centimeters | cm |
| ft | feet | 30 | centimeters | cm |
| yd | yards | 0.9 | meters | m |
| mi | miles | 1.6 | kilometers | km |
| | **AREA** | | | |
| $in^2$ | square inches | 6.5 | square centimeters | $cm^2$ |
| $ft^2$ | square feet | 0.09 | square meters | $m^2$ |
| $yd^2$ | square yards | 0.8 | square meters | $m^2$ |
| $mi^2$ | square miles | 2.6 | square kilometers | $km^2$ |
| | acres | 0.4 | hectares | ha |
| | **MASS (weight)** | | | |
| oz | ounces | 28 | grams | g |
| lb | pounds | 0.45 | kilograms | kg |
| | short tons (2000 lb) | 0.9 | tonnes | t |
| | **VOLUME** | | | |
| tsp | teaspoons | 5 | milliliters | ml |
| Tbsp | tablespoons | 15 | milliliters | ml |
| fl oz | fluid ounces | 30 | milliliters | ml |
| c | cups | 0.24 | liters | l |
| pt | pints | 0.47 | liters | l |
| qt | quarts | 0.95 | liters | l |
| gal | gallons | 3.8 | liters | l |
| $ft^3$ | cubic feet | 0.03 | cubic meters | $m^3$ |
| $yd^3$ | cubic yards | 0.76 | cubic meters | $m^3$ |
| | **TEMPERATURE (exact)** | | | |
| °F | Fahrenheit temperature | 5/9 (after subtracting 32) | Celsius temperature | °C |

*1 in = 2.54 (exactly). For other exact conversions and more detailed tables, see NBS Misc. Publ. 286, Units of Weights and Measures, Price $2.25, SD Catalog No. C13.10:286

### Approximate Conversions from Metric Measures

| Symbol | When You Know | Multiply by | To Find | Symbol |
|---|---|---|---|---|
| | **LENGTH** | | | |
| mm | millimeters | 0.04 | inches | in |
| cm | centimeters | 0.4 | inches | in |
| m | meters | 3.3 | feet | ft |
| m | meters | 1.1 | yards | yd |
| km | kilometers | 0.6 | miles | mi |
| | **AREA** | | | |
| $cm^2$ | square centimeters | 0.16 | square inches | $in^2$ |
| $m^2$ | square meters | 1.2 | square yards | $yd^2$ |
| $km^2$ | square kilometers | 0.4 | square miles | $mi^2$ |
| ha | hectares (10,000 $m^2$) | 2.5 | acres | |
| | **MASS (weight)** | | | |
| g | grams | 0.035 | ounces | oz |
| kg | kilograms | 2.2 | pounds | lb |
| t | tonnes (1000 kg) | 1.1 | short tons | |
| | **VOLUME** | | | |
| ml | milliliters | 0.03 | fluid ounces | fl oz |
| l | liters | 2.1 | pints | pt |
| l | liters | 1.06 | quarts | qt |
| l | liters | 0.26 | gallons | gal |
| $m^3$ | cubic meters | 35 | cubic feet | $ft^3$ |
| $m^3$ | cubic meters | 1.3 | cubic yards | $yd^3$ |
| | **TEMPERATURE (exact)** | | | |
| °C | Celsius temperature | 9/5 (then add 32) | Fahrenheit temperature | °F |

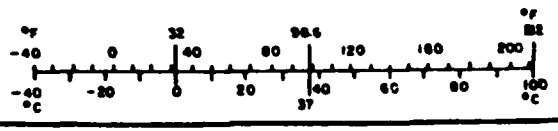


60 mph = 52.1 knots (nautical miles per hour)
60 mph = 88'/sec  1g = 32.2'sec$^2$

1 mph = .87 knots
1 knot - 1.15 mph

TABLE OF CONTENTS

LIST OF FIGURES

## LIST OF FIGURES (Continued)



## LIST OF TABLES



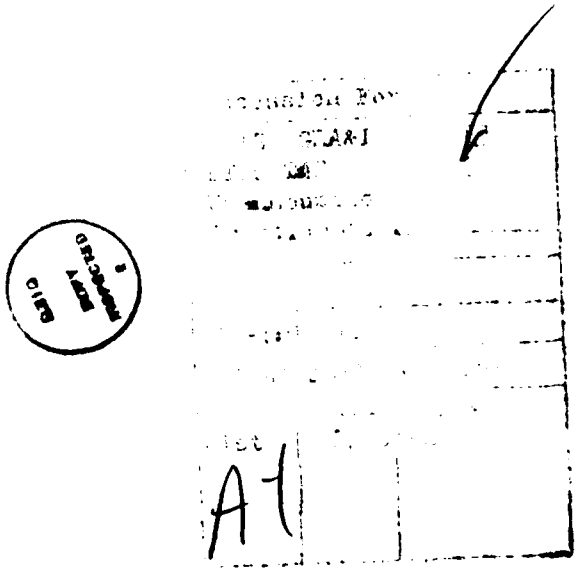

# 1. INTRODUCTION

## 1.1 PURPOSE OF THE STUDY

It is generally known that the wet braking action of an aircraft tire is considerably better on a grooved runway than on an ungrooved runway. Aircraft hydroplaning is eliminated or delayed to higher speeds on runways grooved normal to the flight path. This improved braking performance is believed to be the result of a dual process of water removal from the tire-runway interface. First, the grooves influence the surface water drainage by providing smooth channels into which and through which water can flow freely. Whether decreases in groove spacing will continuously improve the drainage on the runways is not known. The smaller groove spacing will create more flow area and thus more flow per unit length, but a larger spacing might be equally effective and certainly less expensive. Groove spacing, surface texture, and slope of the runway are interrelated in establishing the free flow of water. Second, the grooves provide forced water escape from the tire-runway interface when the aircraft is decelerated on a water-covered runway. Since the maximum amount of water that can be removed from the runway in a given time is limited, both the free flow and forced escape of water are important.

The relative improvement in the braking performance of an aircraft resulting from forced water escape in grooves of various spacings was established in Reference 1. The results indicated that an increase in groove spacing causes reduction in available friction level. The effect of groove spacings on the free flow of water in terms of the water depths on a runway is the subject of the research reported here.

The research was divided into two phases. In Phase I, a mathematical model was developed which included the following parameters: (1) transverse slope of surface, (2) surface texture, (3) groove size and shapes, (4) groove spacing, and (5) uniform rain rate. The model used the kinematic wave approximation to the shallow water equations, for grooved and ungrooved runways with a zero longitudinal slope and a transverse slope of 1.5%. The assumption was made that all rain falling on the pavement drains freely from

the edge of the pavement, except for water that either is stored in grooves or merely contributes to the wetness of the pavement. Grooves were assumed to run through the edge of the pavement; however, the model would handle the commonly occurring case where grooves do not run out to the edge of the pavement. Water can be visualized as spilling out of the ends of these sloping grooves onto the ungrooved portion of the pavement. Flow can then exit from the pavement edge at the same depth it would have on an ungrooved runway. Numerical solutions of the model were generated by a FORTRAN IV computer program. Hydroplaning analysis was not within the scope of this research, even though the results reported here are important to that topic. A discussion of hydroplaning may be found in publications such as Agrawal and Daiutolo [1] and Horne [2].* Phase I has been documented in References [3] and [4].

Phase II constituted the experimental part of the project. This phase incorporated the following elements:

1. Indoor facility using a rain-producing machine developed in a cooperating study sponsored by the Federal Highway Administration, with storm durations and intensities being restricted to those in that study.

2. Portland cement concrete test slab approximately 15 ft (longitudinal) by 30 ft (transversal), the size being restricted by the rain equipment described in (1) above.

3. Sampling from the groove spacing and rain parameters listed for Phase I, for a fixed transverse slope of 1.5% and an as-built concrete surface with 0.25-in.-square grooves only.

4. Determination of time to reach steady state under various rain rates.

---

*Numbers in brackets refer to corresponding items in the list of references.

5. Measurement of water depths and flow rates under steady-state conditions.

6. Modification of the Phase I mathematical model on the basis of the experimental results for rectangular grooves, and extrapolation beyond the range of experimental parameters.

Phase II has been documented in Reference [5].

## 1.2 CONCEPTUAL APPROACH TO THE PHASE I ANALYTICAL MODEL

One-dimensional flow over a sloping, ungrooved section of pavement is relatively easy to visualize. A uniform rainfall begins. Flow and depths over the whole section gradually build up with time and distance downslope (unsteady flow). After a short time, steady-state (equilibrium) conditions are reached at all points on the surface. Application of the equations from the kinematic wave approximation, shown later in detail, occurs smoothly, efficiently, and as accurately as estimates will permit. Maximum values of depth and flow exist at the downstream end of the pavement.

Flow over the grooved pavement is almost as easy to visualize, with unsteady conditions followed by equilibrium conditions. Application of the one-dimensional kinematic wave equations does not occur smoothly, however, since some water will flow laterally into the grooves. This lateral inflow refers to local flow approximately parallel to the flight path. The inflow can be imagined to occur at a faster rate further downstream where larger depths (heads) are available, and will add to the flow the grooves carry due to rain falling directly into them. At some point the grooves fill up, and flow apparently occurs over the surface in a manner similar to that on the ungrooved surface, although at lower depths.

A mathematical model for the grooved pavement was attempted by using a side-channel weir equation to estimate the lateral inflow. Execution of the computer program for this model appeared successful until conservation of mass (continuity) was checked. The flow leaving the pavement was less than the total flow occurring on the pavement due to rainfall. After several

refinements, the error was reduced to 6%, but further study was unsuccessful in eliminating the error and the model was set aside.

A second effort was attempted, in which all of the rain falling on the pavement at the upstream end was compared with the total volume of the grooves to estimate where the grooves were filled. Once this point was established, computations were executed beginning there as though the pavement were ungrooved, except that the flow in the full grooves was accounted for. A small continuity error of about 0.5% was found, perhaps due to round-off error. This model was set aside because it seemed unrealistic. It is difficult to imagine completely filled grooves at the upstream end of the pavement with no flow on the adjacent textured pavement. Also, at the extreme upstream edge, there would not have been sufficient rainwater to fill the grooves.

A third model was developed using the concept of the wetted perimeter, i.e., the total linear length of the solid boundary of a cross section through which flow can occur. The wetted perimeter is the primary factor related to the boundary shear stress caused by the flow of water over the surface. The model assumes a planar ungrooved boundary which has a width equivalent to the wetted perimeter of a grooved boundary, thereby preserving the shear area. For example, in Figure 1 (which shows the sizes and spacings, s, of the two groove patterns considered in this study, as well as the lateral inflow into grooves and the surface depth), the width of the equivalent planar section corresponding to s for the rectangular grooves is (s + 0.5 in). Thus, a segment 0.75 in. in width models the groove on this planar section. Rain still falls into the middle 0.25 in. of this segment, but the rain falling on the additional 0.25 in. on each side of the segment is also considered to be carried in the groove as an arbitrary allotment of lateral inflow from adjacent surfaces. Hence, there is available water to be carried on the adjacent textured surface, but less than on an ungrooved pavement. A computer program executed this model successfully, with continuity exactly satisfied.

This planar model is not without weaknesses. The allotment of lateral inflow into a groove from adjacent surfaces is based solely on how much

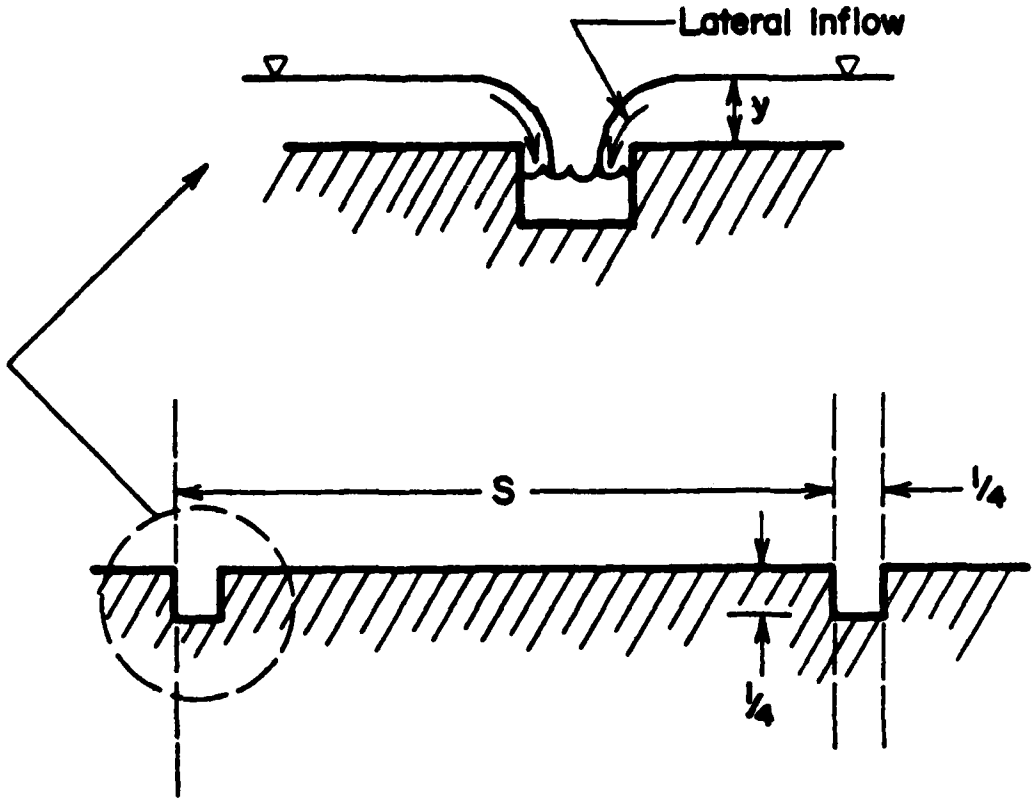


(a) Rectangular groove pattern (dimensions in inches)
s = ∞, 5 in., 2-1/2 in., 1-1/4 in.

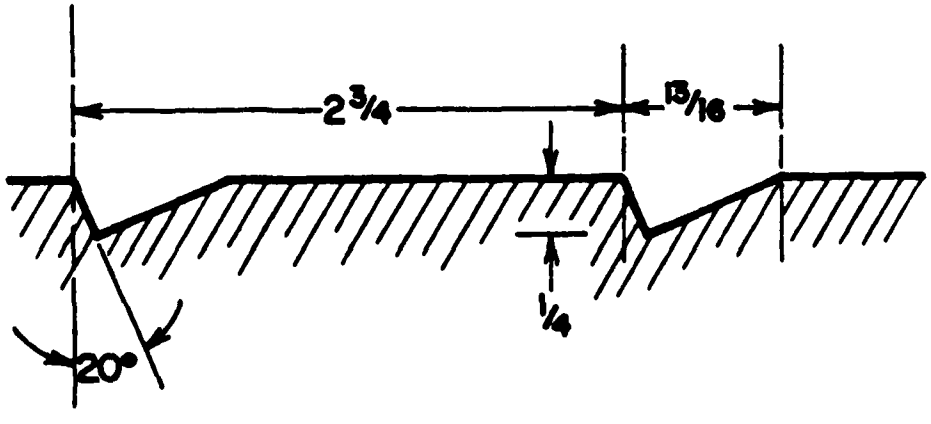


(b) Reflex-percussive groove pattern (dimensions in inches)

Figure 1. Pavement Groove Patterns

larger is the wetted perimeter of a groove compared with its top width. The rectangular groove shown in Figure 1(a) has a wetted perimeter three times its top width; however, the wetted perimeter of the reflex-percussive groove shown in Figure 1(b) is only about 25% larger than its top width. If the region of influence of a groove for lateral inflow is defined as the wetted perimeter minus the top width, then the region of influence for the rectangular grooves is 0.5 in., whereas for the reflex-percussive groove it is only 0.184 in. One would think that the two should be equal, but the arbitrary allotments of lateral inflow to the grooves' shapes will be different. Experimental correction of the mathematical model, however, was rather simple.

There are two other minor problems with the planar model when the model's results are reverted to the actual situation of flow over the grooved pavement. The first is that while the grooves are filling, not all of the wetted perimeter of a groove is shear area. Second, lateral inflow to a groove will continue realistically after the groove is filled up and until the planar model depth is equal to the depth above a groove; but beyond that point, lateral inflow to the grooves must be stopped.

All three conceptual models assumed a constant hydraulic roughness coefficient (Manning's n) across a cross section, even though the rectangular grooves will be shown later to have a lesser value than that of the textured surface as a result of polishing while being grooved. The larger Manning's n value was considered to be conservative for Phase I because it predicted larger depths.

The model based on the concept of wetted perimeter was chosen for both phases of this research. The reasons for selecting it are the ease with which continuity is satisfied and the facility with which adjustments can be made to it based on experimental evidence.

## 1.3 SCOPE OF THE PHASE II EXPERIMENTS

The project called for the construction of an indoor portland cement concrete slab and the provision of all the necessary equipment for runoff

measurements. The slab was built at the Pennsylvania Transportation Research Facilities. Rainfall simulation equipment, developed in a cooperating study for an area 30 ft by 15 ft to provide a rainfall intensity of about 1 inch per hour, supplied the artificial rain. The slab size of 30 ft by 15 ft was a cost-effective accommodation to the rain simulation equipment, since the 30-ft dimension is not typical of the 100-ft transverse width of a runway lane.

The complete project work plan consisted of two rainfall rates (approximately 1 in./hr and 2.5 in./hr) applied to each of the four rectangular groove spacings shown in Figure 1(a). Water depths were recorded at predetermined locations on the slab where sensor openings were connected to pressure transducers. FAA personnel cut the grooves, with their equipment, parallel to the 30-ft dimension. No experiments were to be conducted on the reflex-percussive grooves shown in Figure 1(b), although prediction of their effect on runoff was to be made from the experience on rectangular grooves. The spacing of 1.25 in. has been widely used and formed the basis for the spacings studied. See Reference [6] for a discussion of 3-in. spacing versus 1.25-in. spacing.

## 1.4 RELATION OF PHASE II TO PHASE I

It was anticipated that the experiments would yield information concerning the amount of lateral inflow to grooves, and the hydraulic roughness coefficient for pavement and groove surfaces. A computer program developed to solve the analytical model was modified to accommodate this information. In addition, the modified model was used to generate mathematical water surface profiles to be compared with plotted data points. Finally, the modified model was used to predict runoff depths beyond the 30-ft range of the slab for a variety of conditions of pavement roughness and rainfall rate for the two groove shapes shown in Figure 1.

# 2. ANALYTICAL MODEL

## 2.1 BACKGROUND

The equations for predicting water thickness on an overland flow surface such as a sloping pavement are known as the shallow water equations. These equations are based on conservation of mass and momentum during unsteady, spatially varied flow, and have the one-dimensional form shown in Henderson [7] and Chow [8]:

$$\text{Continuity:} \quad \frac{\partial y}{\partial t} + u \frac{\partial y}{\partial x} + y \frac{\partial u}{\partial x} = q \tag{1}$$

$$\text{Momentum:} \quad \frac{\partial u}{\partial t} + u \frac{\partial u}{\partial x} + g \frac{\partial y}{\partial x} = g(S_0 - S_f) - \frac{q}{y}(u - v) \tag{2}$$

where

$u$ = local velocity in fps
$y$ = local depth in ft
$g$ = gravitational acceleration constant
$q$ = lateral inflow or rainfall excess rate in $cfs/ft^2$
$S_0$ = slope of plane or channel in ft/ft
$S_f$ = friction slope in ft/ft
$v$ = velocity of lateral inflow in ft/s
$x$ = distance downstream in ft
$t$ = time in s

A definition sketch of the variables is shown in Figure 2. Note that x and y are referenced to a horizontal line and not to the sloping line of the plane surface. The difference is negligible for small values of $S_0$. Equations (1) and (2) have been applied to many problems of open-channel flow, including the analysis of flood wave movement in river systems. Their solution on the computer requires the use of complex finite-differencing methods which are time-consuming and sometimes numerically unstable, as Liggett and Woolhiser [9] have indicated.

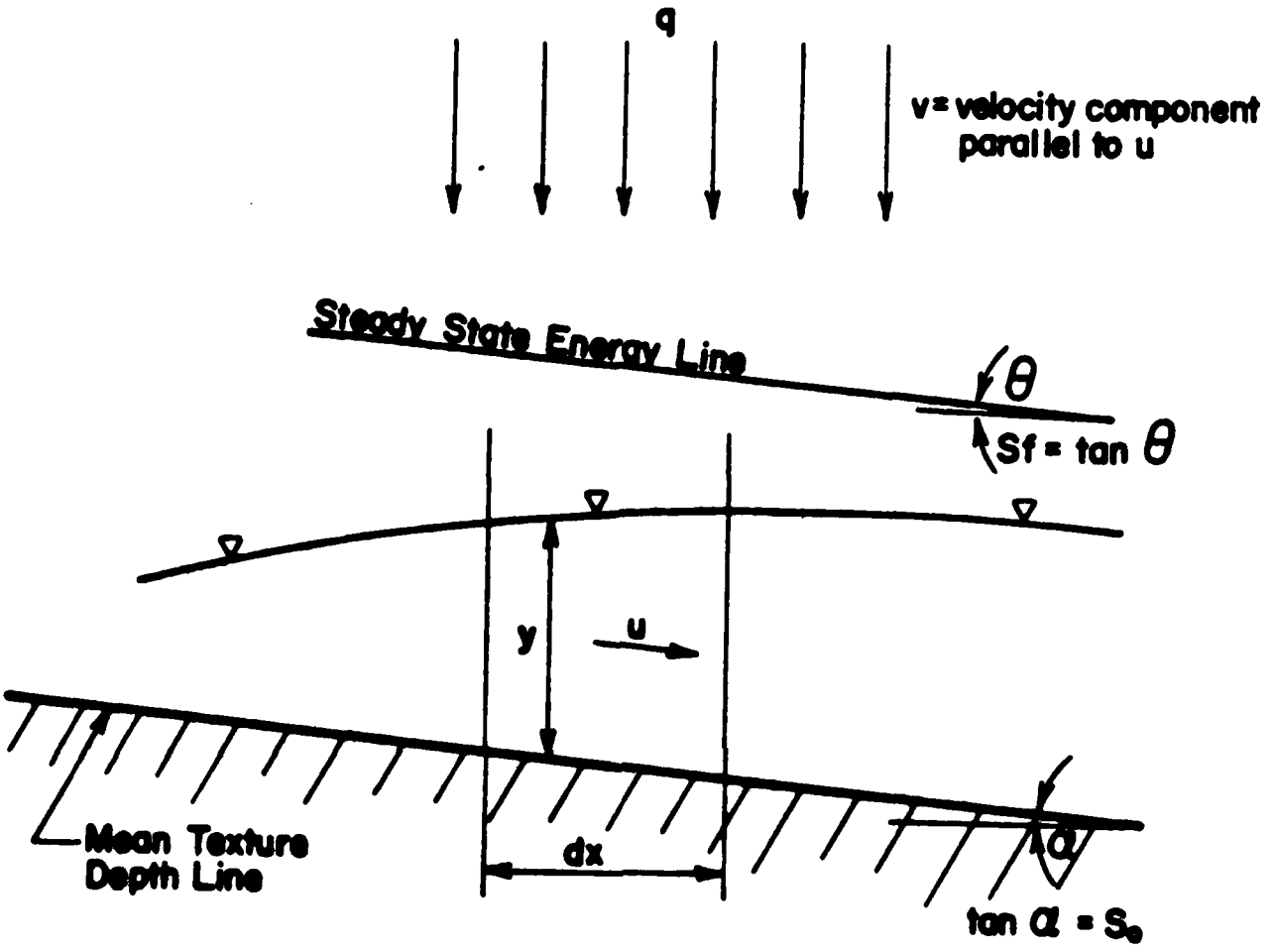


Figure 2. Definition Sketch of Overland Flow on a Plane Surface

As will be shown in Section 2.2, many investigators have examined the properties of the kinematic wave solution as an approximation to the complete shallow water equations. Typical results are given by Lighthill and Whitham [10]. The kinematic wave approximation is generally valid when the friction forces on the plane or channel are assumed to be just balanced by the gravitational forces. Hence, $S_0 = S_f$, and when the slopes disappear from the momentum equation, the resulting absence of force terms implies "kinematic." The ever-changing y in Figure 2, caused by rainfall excess, implies "wave." Under these conditions, the Chezy or Manning formula (described later as equations (6) and (7)) can be used to describe the resulting flow if it is fully rough turbulent, as justified by the condition in equation (11). This situation is usually the case. Woolhiser and Liggett [11] in particular have tested kinematic solutions for the rising hydrograph on an overland flow plane and have concluded that most cases of overland flow can be represented by the mathematically simpler kinematic wave approximation.

Numerous studies of the kinematic wave equation have been completed since the late 1960s, and this simplified approach has been almost universally accepted for the analysis of surface runoff and overland flow from paved surfaces. Kibler and Aron [12] have applied a kinematic wave runoff model to the controlled laboratory runoff studies of Izzard [13] for various pavement surfaces. It can be seen from the typical results of the kinematic wave model shown in Figure 3 that simulated runoff agrees closely with the measured Izzard runoff under changing rainfall supply rates at two different values of hydraulic roughness (Manning's n).

Gallaway, Schiller, and Rose [14] have correctly identified the pavement runoff factors as rainfall intensity, pavement texture, cross slope, and flow length, and have incorporated these into an empirical expression for average water depth above the top of the texture. Although their study is valuable as a background for the present study, it does not account for pavements that are grooved, nor does it indicate a basic measure of flow resistance, such as Manning's n, which is vital to a kinematic wave solution. Reed and Kibler [15] have used data from this and other studies [16, 17] to calculate Manning's n using the equations shown in Section 2.2, and subsequently to

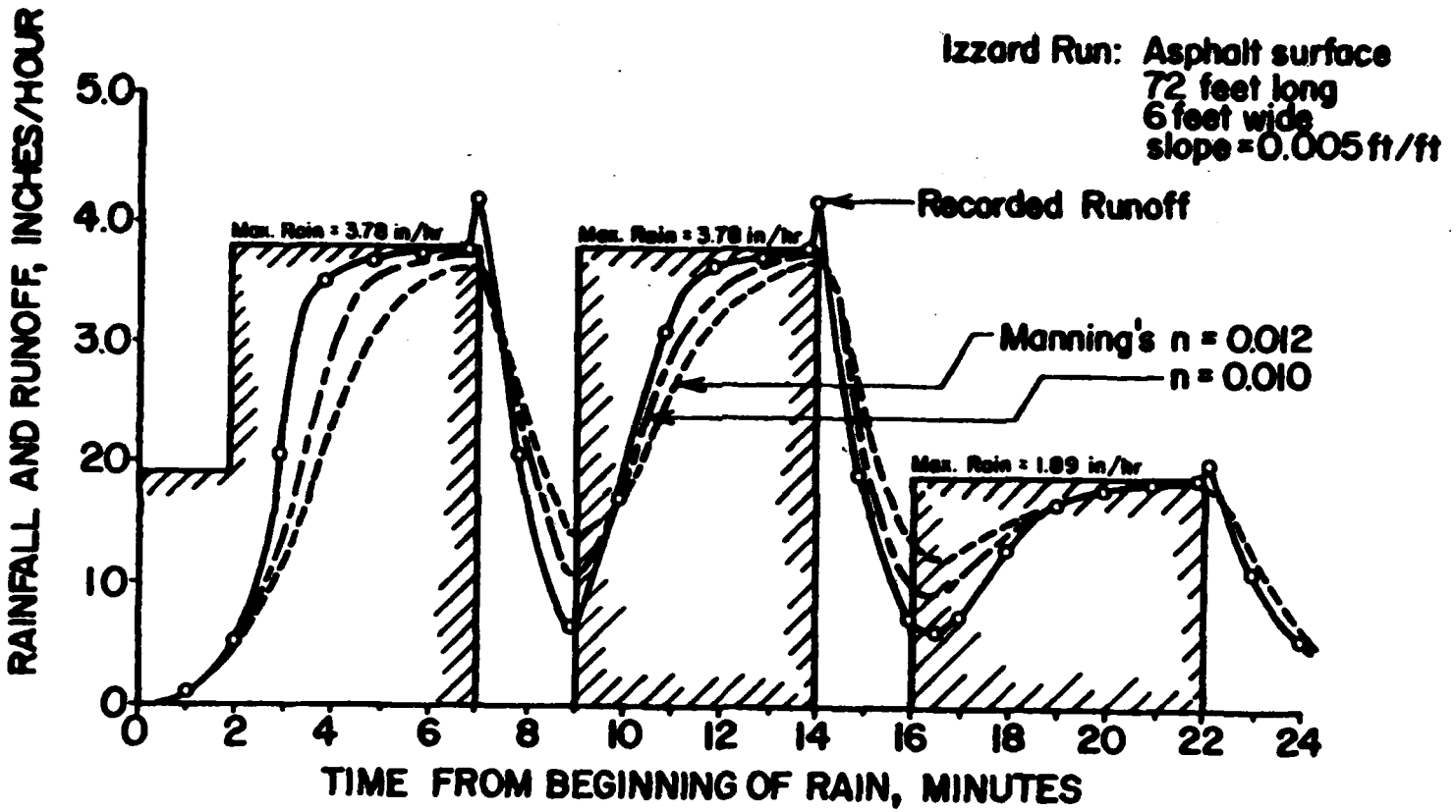


Figure 3. Kinematic Wave Runoff Model Application to Izzard Asphalt Surface [12]

investigate its prediction. Some of their results are shown in Figure 4. The average and upper limit curves of Manning's n values were used in this study to estimate hydraulic roughness. The texture depth can be obtained from macrotexture measurements, which are typically described in Rose et al. [18] and Henry and Hegmon [19]. Representative values of Manning's n were selected initially for the analytical model from typical runway macrotextures between 0.01 in. and 0.03 in; however, measurement of the actual macrotexture of the experimental slab in Phase II was necessary to obtain n from Figure 4 in the early experimental analysis.

In their study, Reed and Kibler [15] have used conditions described in the next section by equations (3) and (11) to justify their use of the kinematic wave approximation as well as the use of the Manning equation. Even in cases where equation (11) might not be satisfied, the flow might still be turbulent because of the turbulence added by pelting rain, a view supported by the Army Corps of Engineers [20].

## 2.2 BASIC EQUATIONS FOR OVERLAND FLOW ON PAVED SURFACES

When rain falls on pavements such as highways, streets, and runways, flow over the surfaces occurs in a form that has become known as urban runoff. This flow is analogous to the flow that would occur in an impervious open channel of very great width, and hence may be referred to as overland flow. The hydraulics of overland flow are generally described by the kinematic approximation to equations (1) and (2). It has been shown [11] that the kinematic wave approximation to these equations is generally valid when the parameter K exceeds 20 and the Froude number, $F_0$, exceeds 0.5, where

$$K = \frac{S_0 \cdot L_0}{H_0 \cdot F_0^2} \tag{3}$$

where

$S_0$ = slope of flow path, ft/ft

$L_0$ = length, ft

$H_0$ = normal depth, ft

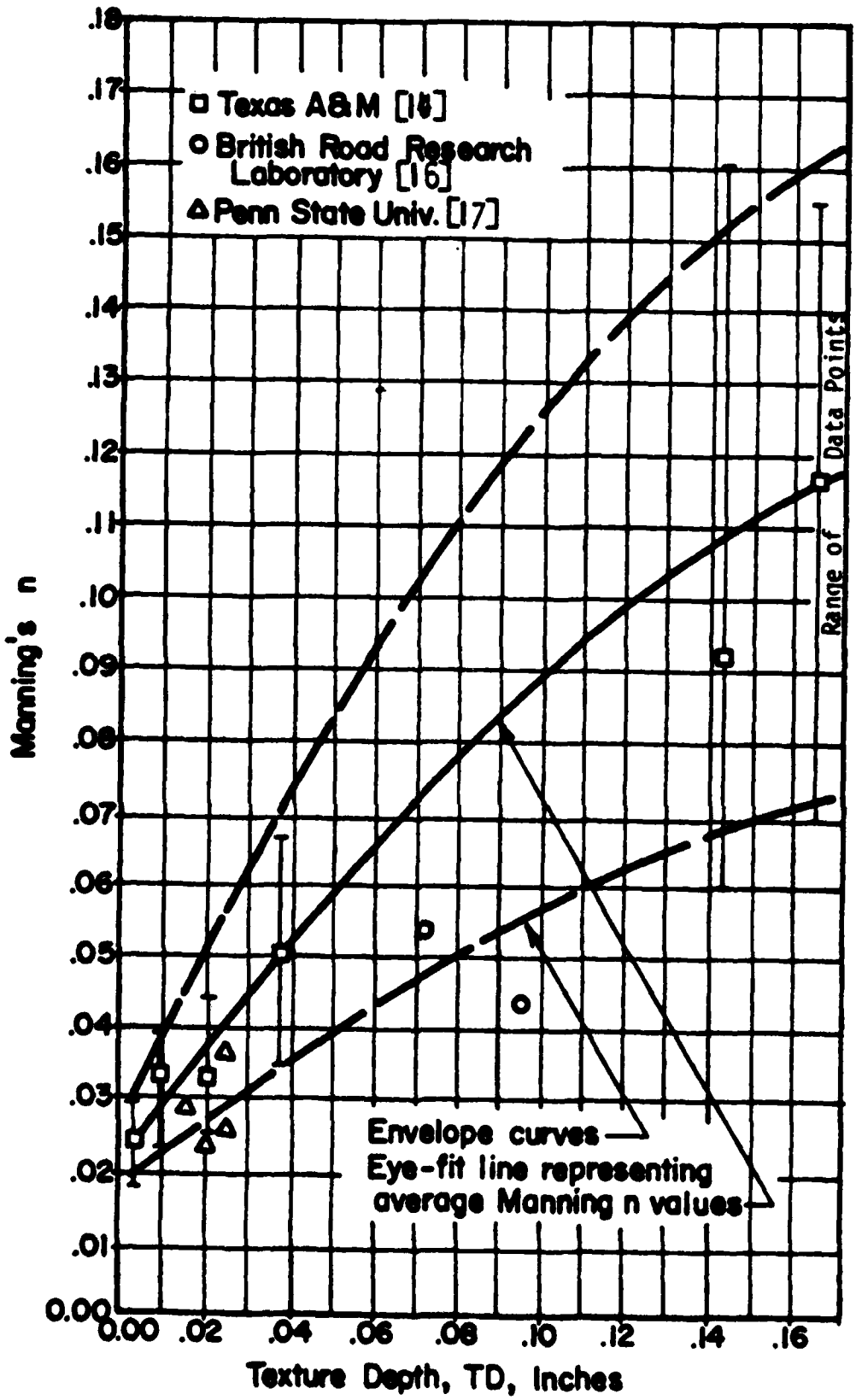


Figure 4. Relationship Between Texture Depth and Manning Roughness Coefficient Based on Measured Water Depths [15]

$F_0$ = Froude number = $V_0/\sqrt{gH_0}$

$V_0$ = normal flow velocity, ft/s = $(q \cdot L_0)/H_0$

$q$ = lateral inflow or rainfall excess rate in ft/s

$g$ = gravitational constant = 32.2 ft/s$^2$

Under subcritical flow conditions ($F_0 < 1$) where $F_0$ is less than 0.5, an additional criterion must be met [21]:

$$F_0^2 K = S_0 L_0/H_0 > 5$$

Except on extremely flat slopes with intense rainfall, most cases of overland flow on paved surfaces, including the ones in this study, will fall easily into the kinematic range based on the preceding criteria. This means that the more complex equations for spatially varied, unsteady flow can be replaced by the simple equations involving mass continuity and uniform flow. The partial differential form of the kinematic equation is well known and has been used frequently for overland flow modeling in urban watersheds [22]. Integrating the characteristic equation in an x-t plane under constant rainfall condition yields a simple relation for the equilibrium flow depth ($Y_{eq}$) at different points in the downstream direction:

$$Y_{eq} = q\, t_{eq} \tag{4}$$

where

$q$ = lateral inflow or rainfall excess rate in cfs/ft$^2$

$t_{eq}$ = equilibrium flow time, s

The equilibrium flow time, $t_{eq}$, on an impervious surface under constant rainfall excess rate, $q$, is determined by the equation:

$$t_{eq} = \frac{1}{q}\left[\frac{Lq}{\alpha}\right]^{1/m} \tag{5}$$

where

$L$ = length along flow path or width of runway, ft

$\alpha$, $m$ = parameters of the hydraulic friction relationship

Under kinematic flow conditions, the friction or energy slope, Sf, is equal to the slope of the plane, $S_0$, and this permits the use of a simplified uniform flow velocity relation of the form:

$$V = \alpha Y^{m-1} \tag{6}$$

where

V = normal flow velocity, ft/s

Y = flow depth, ft

For uniform turbulent flow on an overland surface, the parameters $\alpha$ and m can be determined from the Manning equation as

$$\alpha = \frac{1.49}{n} S_0^{0.5} \text{ (English units)} \tag{7}$$

$$m = 5/3 \text{ (dimensionless constant)}$$

Equations (4), (5), (6), and (7) provide the theoretical basis for the flow model described earlier in Section 1.2.

Under the assumption of turbulent flow, equation (7) can be applied to equation (5) for $t_{eq}$ to obtain

$$t_{eq}(\text{sec}) = \frac{56.25\, L^{0.6} n^{0.6}}{i^{0.4} S_0^{0.3}} \tag{8}$$

where

i = rainfall intensity in in./hr

n = Manning roughness coefficient

and the other terms are as defined earlier. Equation (4) for $Y_{eq}$ can now be written

$$Y_{eq}(\text{in.}) = \left[ \frac{n\, L\, i}{1023\, S_0^{0.5}} \right]^{0.6} \tag{9}$$

Discharges under uniform rain can now be computed for all points L ft downstream using

$$Q = \alpha\, Y^m \tag{10}$$

where Q = discharge, cfs/ft, and the other terms are as defined earlier. Equilibrium flows can also be obtained from continuity considerations by calculating the inflow onto the pavement upstream from intensity. Equations (8), (9), and (10), together with (6) and (7), provide the computational basis for the FORTRAN IV program written to execute the flow model.

Henderson [7] has suggested that fully rough flow conditions prevail when

$$n^6 \sqrt{R_h S_f} > 1.9 \times 10^{-13} \tag{11}$$

where

$R_h$ = hydraulic radius (assumed equal to overland flow depth, Y)

$S_f$ = friction slope ($S_f = S_0$) under kinematic flow conditions

Equation (11) is satisfied in the present study for most of the data, allowing for some reasonable minimum depth such as 0.02 in. Hence, the use of the Manning equation to describe the friction relations for the pavements in this study is justified. For Henderson numbers less than $1.9 \times 10^{-13}$, the flow is transitional or laminar, and consequently Manning's n should not be used unless it includes the Reynolds number [23].

## 2.3 COMPUTER SOLUTIONS OF THE ORIGINAL MODEL

A FORTRAN IV program was written to solve the mathematical flow model.

The program was executed on an IBM 370/Model 3033 system to generate flow profiles which can be depicted graphically. Several graphs were produced for a wide range of values of the pertinent parameters. These graphs are shown in Reference [3], but they are not completely reproduced here because of the eventual modification of the model from experimental experience, particularly with grooved pavement. However, two of the graphs are shown in Figures 5 and 6. These curves show that increasing rainfall rate and Manning's n values increase water depths on ungrooved runways. The curves are valid for the values of the parameters shown, despite later modifications to the model. The figures were plotted using a Hewlett-Packard graphics terminal which selects appropriate scales for the axes. The scales are not always convenient from the standpoint of good plotting practice. Axes are labeled in word descriptions for clarity.

Note that the maximum rainfall rate of 4 in./hr in Figure 5 was not the maximum considered in plotting some of the other graphs (not shown). That maximum was 6 in./hr, which was chosen because, together with the length of the flow path (which is related to rainfall duration), it statistically represents a storm with a return period of about 25 years in Pennsylvania. Such a storm is typically used to estimate design flows for storm drainage systems. Unfortunately, the rain equipment used in the experiments in Phase II has a limiting output of about 3 in./hr. Hence, that value was used for predictive analysis later.

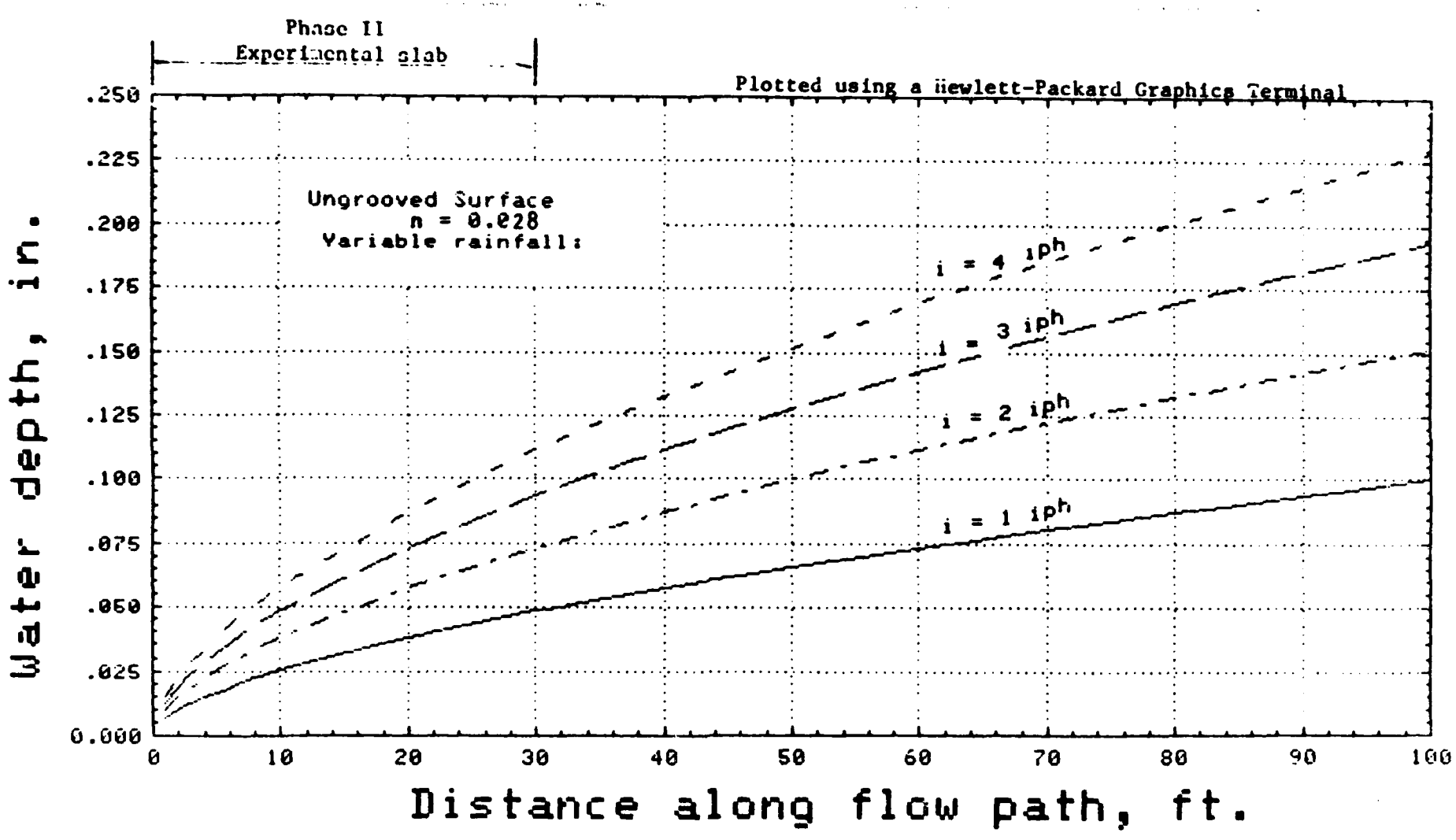


Figure 5. Effect of Variable Rainfall Rate on Water Depth, $Y_{eq}$, for Ungrooved Surface

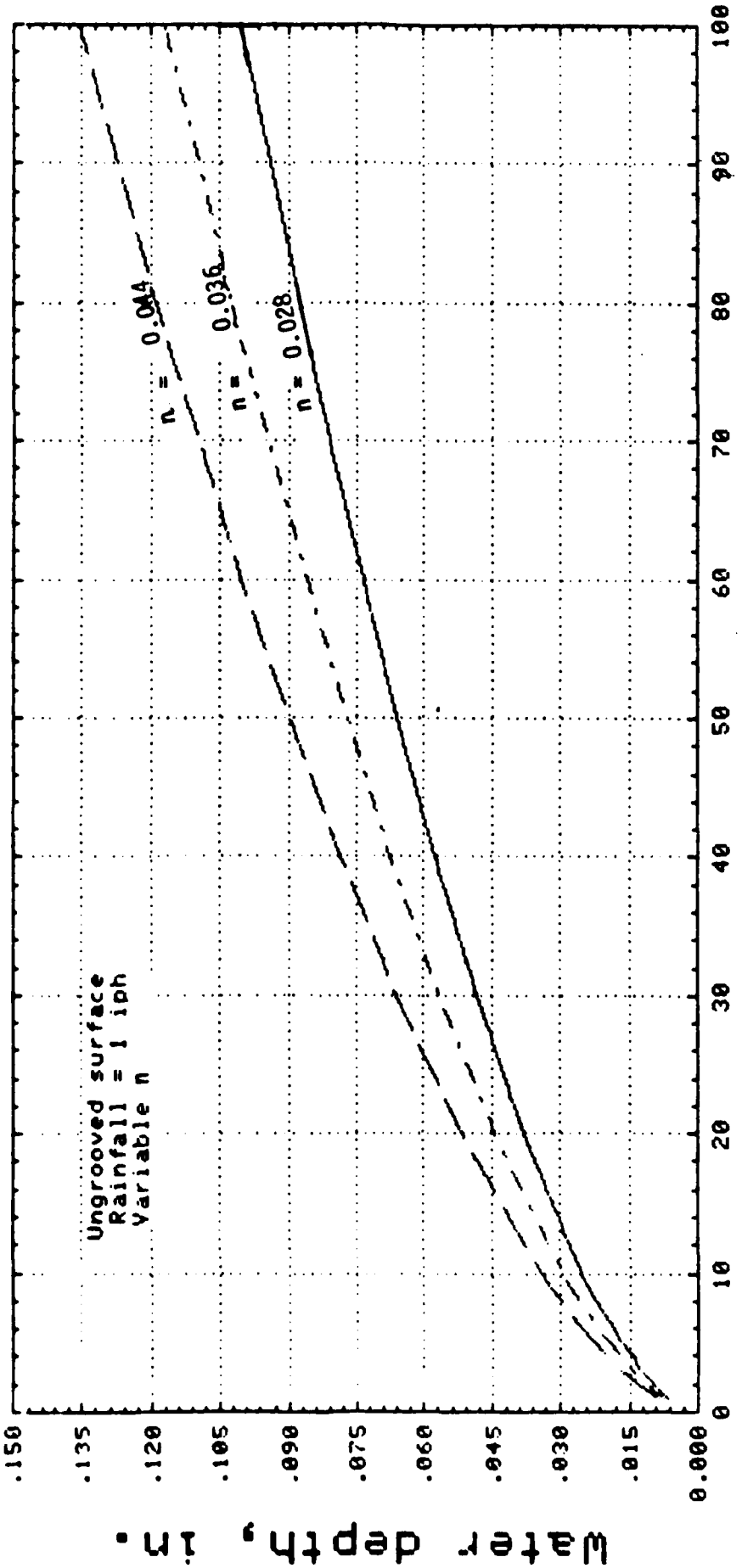


Figure 6. Effect of Variable Manning Roughness, n, on Water Depth, $Y_{eq}$, for Ungrooved Surface

# 3. EXPERIMENTAL SYSTEM

## 3.1 CONCRETE SLAB AND ARTIFICIAL RAINFALL

The concrete slab was constructed to be 4 in. thick with light reinforcing to minimize tension cracks. A plan view is shown in Figure 7. The slab slopes along the 30-ft dimension at 1.5%. The slope was set accurately on the concrete forms prior to construction, using precise surveying equipment. It was checked again after the concrete had been poured, typically finished with a stiff broom in the 30-ft direction, and had hardened. The slab was set on a raised pad of crushed limestone aggregate embedded with polyvinyl choride (PVC) pipes as shown, with the top of pipes at the aggregate pad surface. The black dots shown over the PVC pipes in Figure 7 are 3/8-in. holes drilled through the slab to the empty PVC pipes to accommodate instrumentation tubing beneath the slab. The weir box was used to measure the flow off the downstream edge of the pavement. When this flow was compared with the inflow through the rainfall simulator, an estimate of the loss of runoff due to overspray or flow off the side edges of the slab could be made. This comparison is not reported here, since it is not considered relevant to this study.

Figure 8(a) shows a sand-patch test being conducted on the finished ungrooved surface of the slab to determine an average texture depth at a given location. Fifteen such tests were performed uniformly on the surface of the slab, and the results showed an average texture depth of 0.026 in., with a range of 0.022 in. to 0.029 in. The texture depth, in conjunction with Figure 4, provides an estimate of the hydraulic roughness coefficient. A special sand-patch test was made near the center of the slab, where a rather severe blemish occurred in the broom finishing of the fresh concrete. The test showed the blemish to have an average texture depth of 0.048 in. The blemish runs throughout the 15-ft dimension of the slab and can be observed in the photograph in Figure 13(a), shown later in this report.

The photograph in Figure 8(b) shows an overall view of the experimental system in operation, with artificial rain falling on the grooved slab. Eight tripods support the spray nozzles, valves, and pressure gages of the rainfall

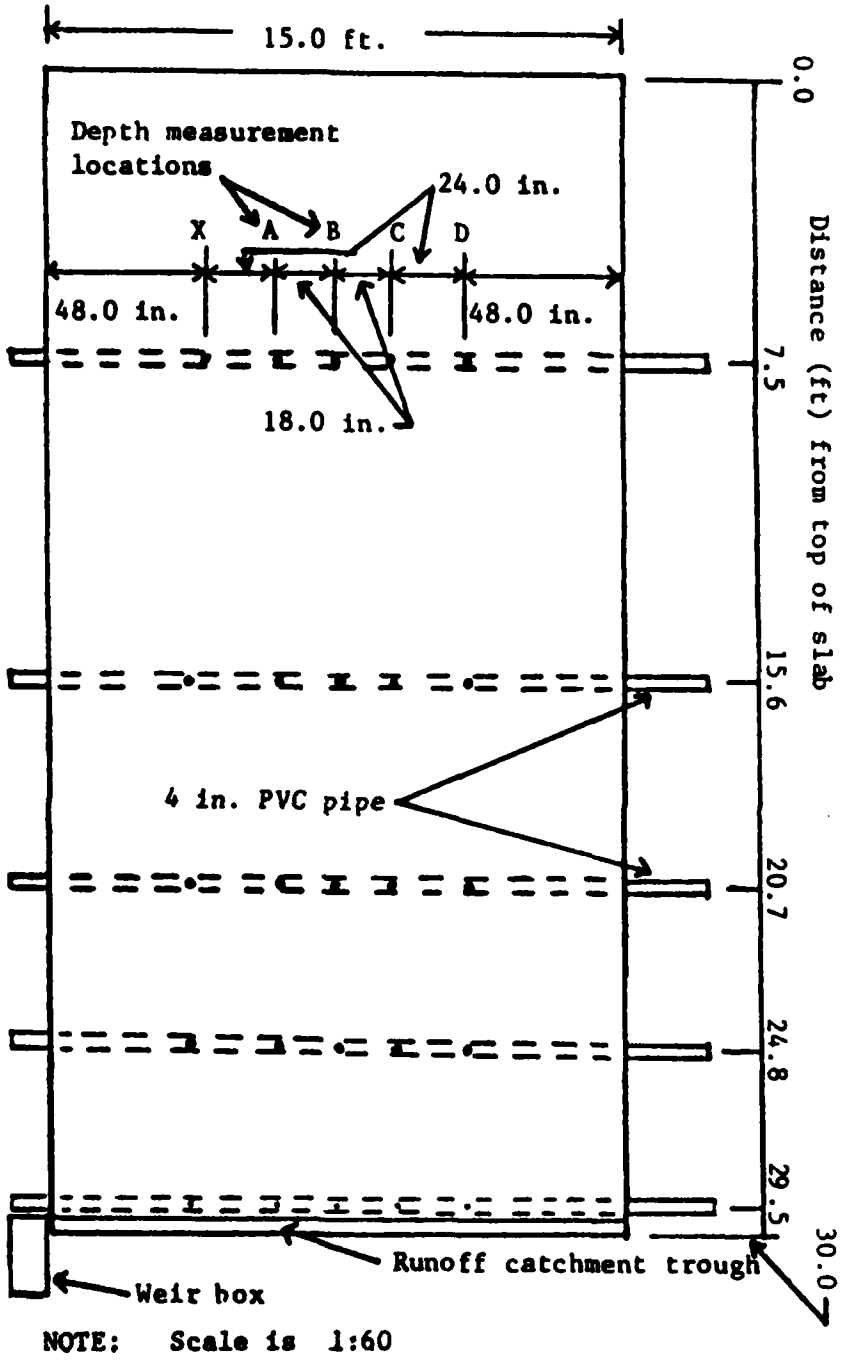


Figure 7. Plan View of Concrete Slab Showing Construction Details

(a) Sand patch test on the dry ungrooved slab

(b) Grooved slab under artificial rainfall

Figure 8. Photographs of the Concrete Test Slab and Artificial Rain Equipment

simulation equipment. A 600-gallon tank truck supplies water to the system. Tank capacity can be a limiting factor in the duration of testing. At the extreme left center of the photograph, a tripod may be observed standing partially on the slab. This condition was created by an error in the slab location. The slab was not placed far enough away from the wall to provide space for setting up a tripod. The error posed no difficulty in the experiments except for voiding the use of the column of sensor openings marked "X" in Figure 7. Also, fewer grooves were cut on that side of the slab. Figure 9 shows the grooves being cut by FAA personnel using a diamond-tipped saw machine.

The rainfall simulation equipment has been documented by Davis [24]. To establish an intensity of 1 in./hr, four nozzles in a predetermined pattern were used, and the pressure gages at the nozzles were regulated to 12 psi. For 2.5 in./hr, eight nozzles were used, and the pressure gages were set at 20 psi. It should be understood that these rainfall rates are spatial averages and not absolutely uniform. Standard deviations in these averages could be about ±0.3 in./hr. To ensure a closer estimate of the rainfall intensities in this research, collection cup data similar to those taken by Davis were taken in the important flow regions spanned by the sensor holes on the slab. These cups may be seen in Figure 10(a), along with a sensor opening shown at the tip of the pen on the textured slab surface. The collection cup data more accurately defined rain rates for this study. These rates were 1.15 in./hr and 2.45 in./hr. Standard deviations were not determined for these averages, but experience has shown that cup data collected in the center of a rained-on area are more nearly uniform. Figure 10(b) is a photograph of the broom-finished surface, showing a rectangular groove and a more discernible 3/8-in. sensor opening.

## 3.2 PRESSURE TRANSDUCERS

Figure 11(a) shows the flexible tubing connected to the sensor openings, emerging from beneath the slab in a 4-in.-diameter PVC pipe. Figure 11(b) shows one of the tubes being connected to a pressure transducer. Ten of these U.S.-made transducers were purchased for this study because their cost

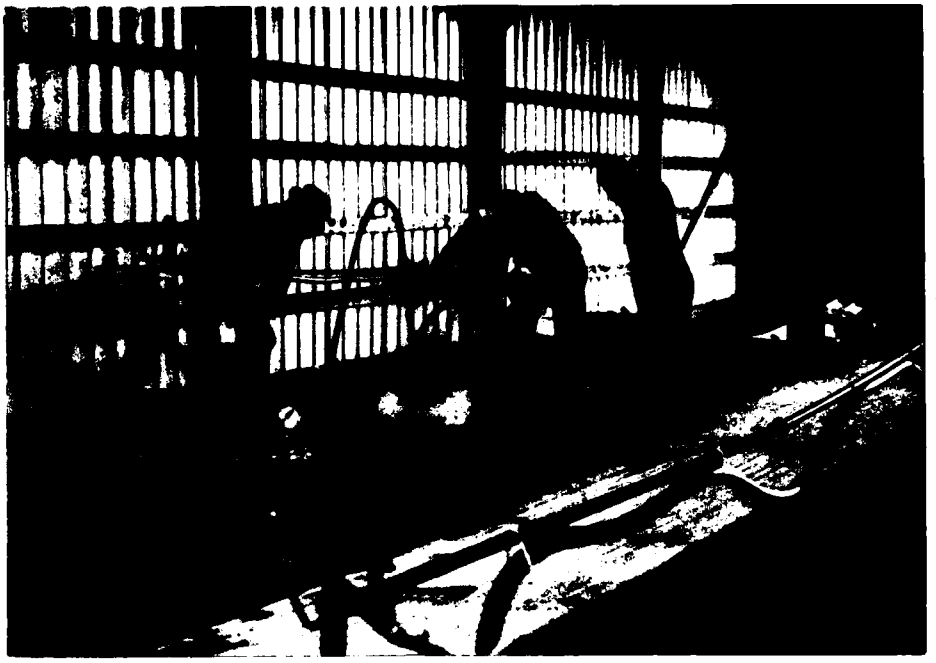

(a) Grooving the slab

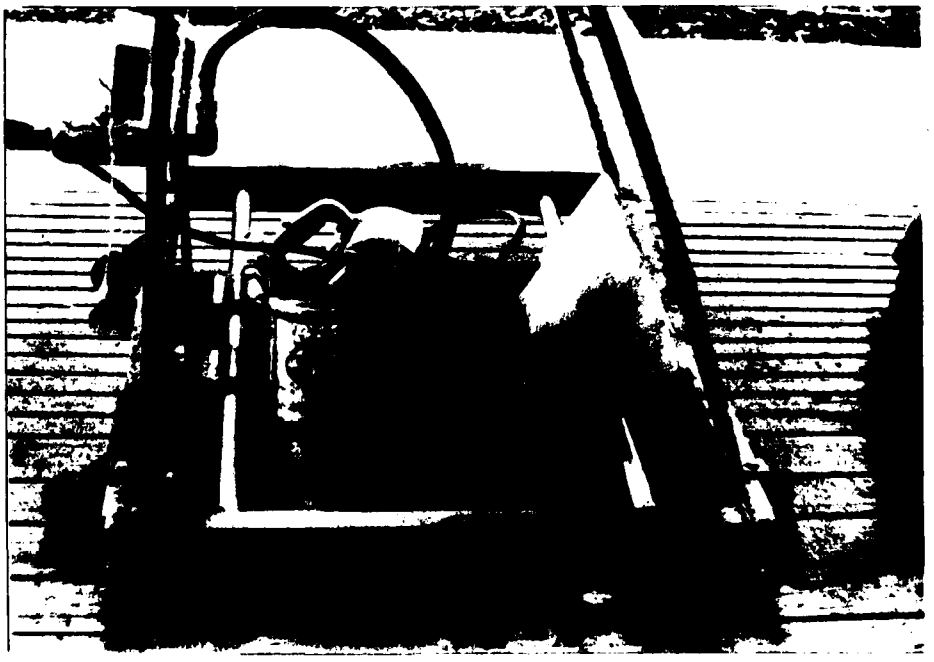

(b) Close-up view of circular saw

Figure 9. Photographs of Grooving Machine in Operation

(a) Collection cups and sensor opening

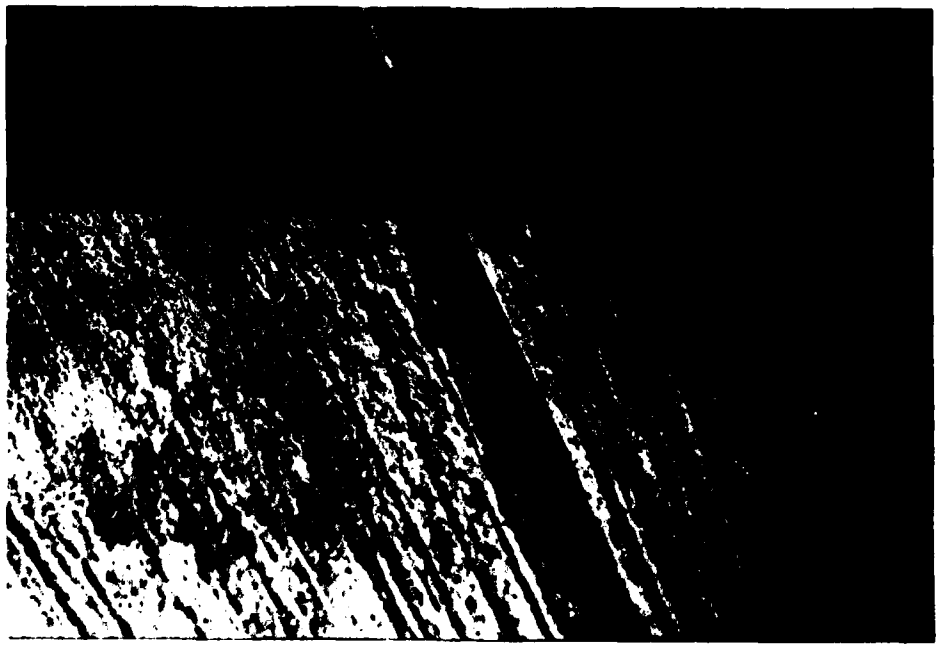

(b) Rectangular groove and sensor opening

Figure 10. Photographs of Textured Surface of Slab Showing Collection Cups, Sensor Openings, and Rectangular Groove

was comparable, without sacrifice of accuracy, to the single one made in Europe and proposed initially for these experiments. In Figure 8(b), the wooden box in which the transducers are mounted can be seen (left center) resting on the floor at the side of the slab. All the transducers were placed below the slab surface to register positive pressures, since they were calibrated for positive pressures in this study. The transducers sense small changes of pressure in the tubing (flow depths on the surface of the slab) and send an electrical signal to a digital multimeter. A 5 volt DC power supply device in the form of a function generator was used with the system. The multimeter was a Data Precision Model 258, with an LCD readout to the nearest 0.01 mV.

Appendix A contains technical data on the pressure transducers, including the calibration coefficients (K) determined individually for the transducers in this study. Figure 12 shows the linear nature of the data, which determines the maximum and minimum K values (slopes). The transducers were calibrated using a container with a bottom opening to which a transducer could be connected. Water levels in the container were varied, and changes in voltage response by a transducer were recorded against changes in water depth measured by a mechanical point gage precise to 0.001 ft.

The depth-measuring system using pressure transducers is considered superior to any system that is mounted either above or on the slab surface. Surface systems can obstruct the very quantity they are intended to measure. One of the disadvantages of transducers is that their sensor positions are fixed. Reference [14] describes an excellent above-the-surface system involving a point gage with a variable (x,y) position.

## 3.3 EXPERIMENTAL PROCEDURE

Two types of experiments were conducted: quantitative experiments which involved the recording of numerical data, and qualitative ones which involved the observation of water movement patterns on the slab, made by a fluorescein dye. Some quantitative work also involved dye.

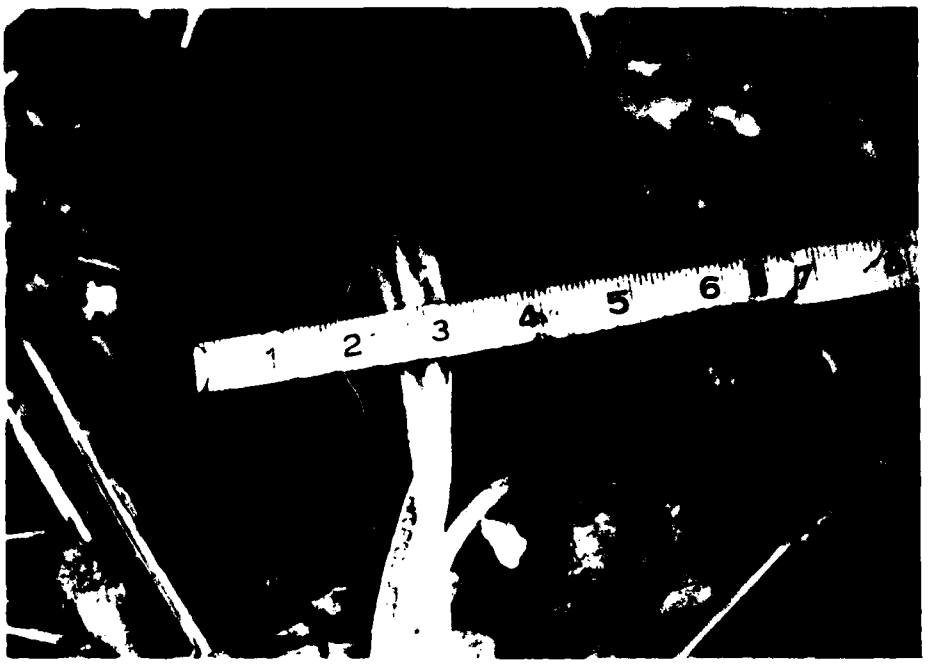


(a) Flexible tubing emerging from PVC pipe

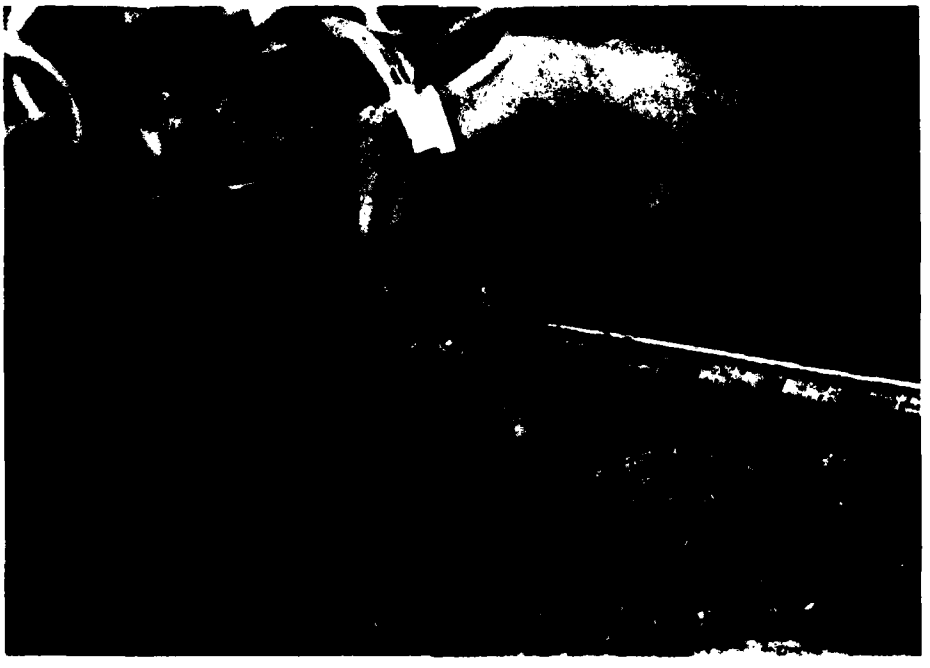

(b) Pressure transducer connected to sensor tubing

Figure 11. Photographs of Connection of Pressure Transducers to Sensor Openings Using Flexible Tubing

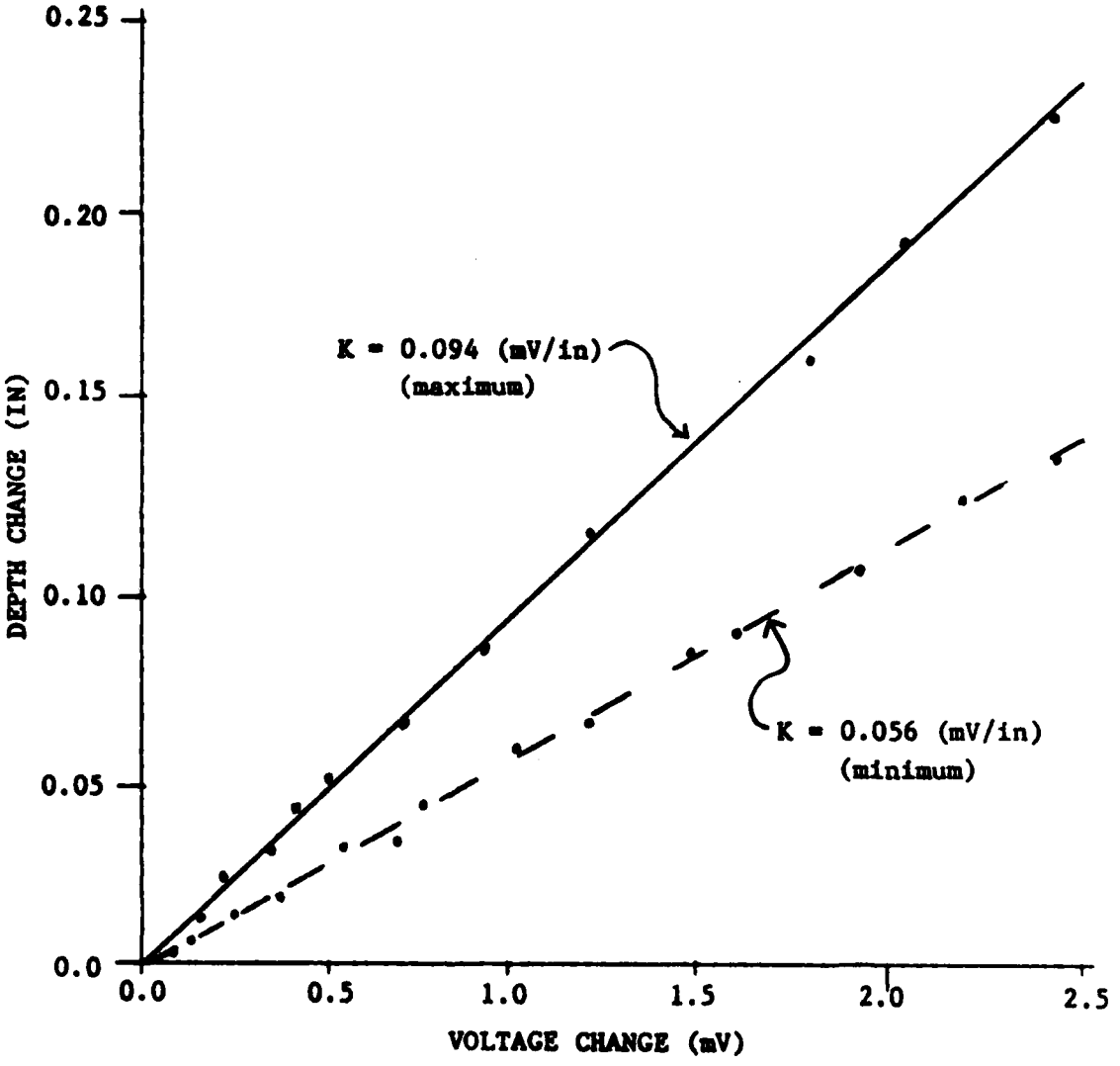


Figure 12. Depth versus Voltage Curves for Pressure Transducers (see Appendix A)

### 3.3.1 Equilibrium Water Depth and Hydraulic Roughness Data

Prior to activation of the artificial rainfall, the tubes connecting the transducers to the slab sensor openings were checked to see whether they were filled with water and had no air pockets. This procedure is difficult because much of the tubing is concealed in the PVC pipes. It is even more difficult for the upstream row of sensors (7.5 ft in Figure 7), where depths are extremely small and as much as 25 ft of tubing is connected to the sensors. The water level in the sensor openings in the slab was then checked, and a judgment was made as to when the level was at the average texture depth datum. In this process a wetting agent in the form of a mild detergent was placed on the opening with an eye dropper in order to break down surface tension and reduce capillarity effects. When the water levels were judged to be at the proper datum, the transducers were zeroed for this level by recording their output voltage. At this point, the rainfall equipment was prepared for an experiment.

With the upstream valves of all eight nozzles of the rainfall simulation equipment closed, the centrifugal pump on the tank truck was started, which applied pressure to the system supplying water to the nozzles. The pipes of translucent material were checked for air pockets, which were then purged through small bleed valves with a minimum loss of water. Then, each nozzle was set for the appropriate pressure by opening the valve, adjusting the pressure regulator, and closing the valve. Again, the loss of water is minimized because this operation takes only a few seconds. When all the nozzles were set, the pump was turned off. The valves to all of the nozzles were opened, and a small residual spray occurred for a short time because of the release of pressure. Testing began when the pump was started and the required intensity sprayed forth. For the tests reported here, the truck capacity provided adequate durations of rainfall, particularly with the conservative startup procedure. A fully running system could purge itself of air as well as have its pressures set; however, the amount of water in the tank when testing began might be very inadequate.

Equilibrium water depth data are given in Appendix B for the ungrooved surface and the grooved surfaces. (Voltage drops were converted to depths

prior to being recorded in the tables; see Appendix A.) The data were recorded as average depths at locations indicated in Figure 7. A range of data values is shown for each depth and was determined by three or more independent depth measurements over several runs. Data were not recorded for the upstream row of sensors at 7.5 ft. There was no discernible depth for the grooved pavement there, and, although some depth could be sensed for the ungrooved pavement, the readings were considered unreliable. Moreover, there are no data shown in Appendix B for grooves spaced at 2.5 in. under rainfall of 1.15 in./hr, or for grooves spaced at 1.25 in. under rainfall of 1.15 in./hr or 2.45 in./hr. Repeated measurements for these conditions resulted in no measurable water depths anywhere on the slab surface.

The measured water depths for the ungrooved pavement appear appreciably larger than the depths obtained from the mathematical model of Phase I. A possible reason for this discrepancy is the uncertainty in the value of the hydraulic resistance coefficient, Manning's n, used in the mathematical model. If the average texture depth of 0.026 in. is used, Manning's n from Figure 4 is 0.042 for the median line and 0.056 for the upper limit line. If the texture depth of 0.048 in. is used for the finishing blemish mentioned earlier (see Figure 13a), the upper limit line of the curve yields n = 0.081. Of course, the blemish occurs only in one area of the pavement, but it extends all the way across the slab. It was decided, therefore, to make a dye trace determination of Manning's n prior to grooving the pavement. For this determination, the time to reach equilibrium conditions at the downstream edge of the slab is customarily approximated by the travel time of the dye over the entire length of the slab under equilibrium conditions. Manning's n was obtained by solving equation (8). The results are shown in Table 1. The n value of 0.096 seems high, but Reference [25] indicates that n might be between 0.05 and 0.15 for water depths comparable to those reported here. Also, in a separate and as yet unpublished thesis study not involving dye or rain, n varied from 0.03 to 0.10 at a fixed location on the slab surface. Hence, the n values used here are compatible with those reported elsewhere.

Not suprisingly, the water depths shown in Appendix B are lower for grooved pavement than for the ungrooved pavement. However, there are no surface depths upstream, a result which is in disagreement with the unadjusted

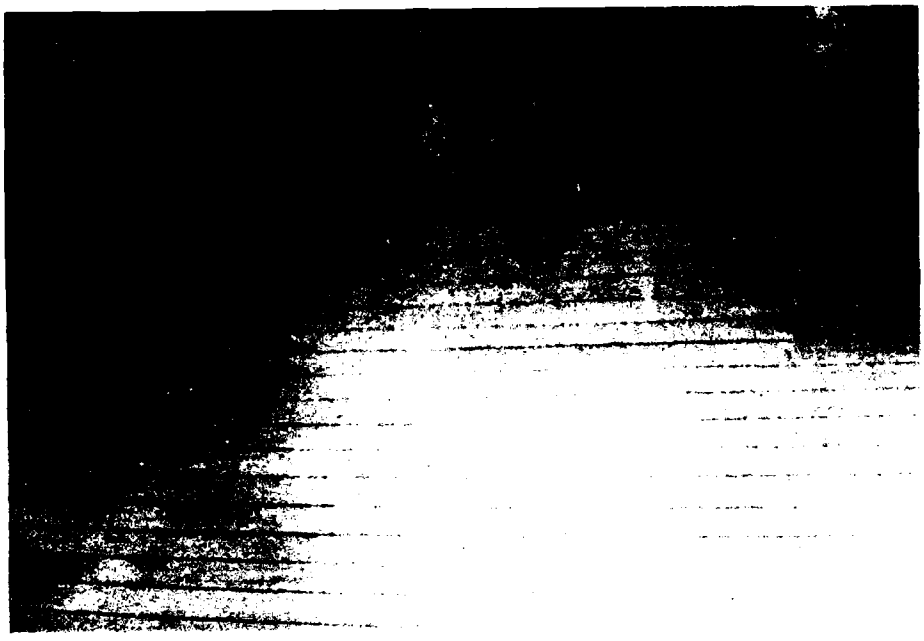

(a) Dye at upstream end of slab

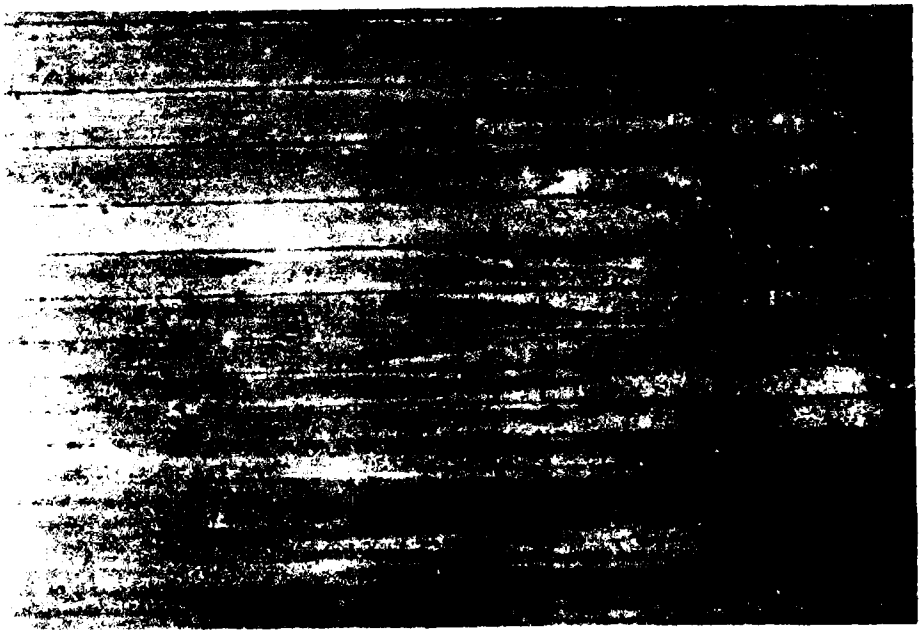

(b) Dye emanating from grooves for flow to the right

Figure 13. Dye Movement with Rainfall on the Grooved Slab

Table 1. Dye Test Results: Determination of Manning's n for Ungrooved Surface

(Distance = 30 ft; slope = 0.015)

| Rainfall Intensity: 1.15 in./hr | | Rainfall Intensity: 2.45 in./hr | |
|---|---|---|---|
| Trial | Equilibrium Time (sec) | Trial | Equilibrium Time (sec) |
| 1 | 347 | 1 | 255 |
| 2 | 362 | 2 | 259 |
| 3 | 349 | 3 | 267 |
| Average | 353 | Average | 260 |
| n = 0.096 | | n = 0.096 | |

Table 2. Test Results: Determination of Manning's n for Grooves

(Distance = 15 ft; grooves flowing full)

| Trial | Travel Time (sec) |
|---|---|
| 1 | 21 |
| 2 | 23 |
| 3 | 24 |
| 4 | 23 |
| 5 | 20 |
| 6 | 21 |
| Average | 22 |

$n_g = 0.0097 \approx 0.010$

mathematical model. This condition suggested that qualitative dye tests be conducted to confirm that all the rain upstream was being carried in grooves, and that quantitative dye tests be run to determine Manning's n for grooves. The qualitative tests are discussed in the next section.

A small study was undertaken to determine n values for groove surfaces, which are polished to some degree by the cutting process. A flow was created from a hose laid on the surface of the grooved slab which was not subject to rainfall. The flow was adjusted so that reasonably long stretches of the grooves would flow full without overflowing onto the surface. The Manning equation, which is represented by equations (6) and (7) for a modeled groove in the Phase I model, can be solved for n if the flow velocity can be measured. Velocities were measured by timing the movement of a tiny piece of styrofoam moving in the grooves over a distance of 15 ft. The results of these measurements are shown in Table 2. The $n_g$ value of about 0.010 is not surprising, since a table look-up for such a surface might show a value of that magnitude.

### 3.3.2 Qualitative Tests Using Dye

A series of dye tests was undertaken to observe water movement on the grooved slab. The dye used was a dark-red powder which becomes greenish-yellow when dissolved in water. The dye may be used in dry or liquid form, but the most effective observations in this study were made by placing the powder along the upper edge of the slab and allowing the rainfall to pick it up and diffuse it downstream.

Two of the color photographs taken during these tests are shown in Figure 13. The left side of Figure 13(a) shows the dye being dispersed at the upstream end of the slab. Very little dye is visible on the surface in the middle of the photograph, indicating that the water is being carried in the grooves. On the right side, dye appears to be coming out of the grooves onto the surface, which indicates that the grooves are filled and overflowing. The surface blemish is evident in Figure 13(a) and is probably the chief cause of the dye emanating from the grooves at that location. The blemish can be considered an undesirable obstruction that slows and ponds the runoff. Figure

13(b) is more typical of the results of this research A closeup photograph of a more uniform section of the slab shows, on the right, dye diffusing out of the grooves because they are filled by all of the inflow upstream. Motion pictures of the experiments were also taken, and are in the posession of FAA personnel at the Technical Center in New Jersey.

The most significant observation from these dye tests was that all the rain falling on the upstream end was carried in the grooves in such a way that the slab surface, although wet, had zero water depth. The width of the area contributing lateral inflow to the grooves would be equal to the groove spacing for spacings of 5 in. and less. At what larger spacing this condition would cease to occur is uncertain. By programming this condition into the computer model, it will be possible to predict the location where the grooves begin to overflow and surface depths again start to build up.

# 4. ANALYSIS OF RESULTS

## 4.1 MODIFICATIONS TO THE COMPUTER MODEL OF PHASE I

The FORTRAN IV computer program, discussed in Section 2.3, was modified to reflect the experience gained from the experiments described in the previous chapter. The Manning's n value used in Phase I for the pavement surface was lower than the experiments have indicated, but since it was an input value to the original program, no program modification was necessary. However, the program was modified to accept as input a separate Manning's n value ($n_g$) for grooves. Another modification to the program was based on the concept that all of the rain falling at the upstream end of the grooved pavement is carried in the grooves and not on the surface. This condition continues until the grooves fill up at some point downstream. At that point, the pavement surface water depths begin to be computed as though flow were occurring over a plane surface with constant n. The program assumes that all rain falling on a spacing of 5 in. or less contributes lateral inflow to a groove. The Phase I computer program used the wetted perimeter of a groove as an arbitrary determination of the rainfall contributing to flow in the groove. While the wetted perimeter concept remained the basis of the model quantitatively, the original computer program was modified to use the actual geometry of grooved pavement because there was no flow on the upstream pavement surface. The nature of this model made adjustment to actual conditions easy by incrementally comparing rain volume rates to groove flow downstream to determine the point where the grooves overflow. The origin of L in equation (9) is then shifted to this point for subsequent computations of water depths on the pavement surface.

The flow diagram, listing of statements, guide to input, and typical output of the modified computer program are presented in Appendices C, D, E, and F, respectively. The program was executed on an IBM 370/Model 3033 system. The modified model results are shown graphically in this chapter. The Manning's n values shown on graphs from this point on are those for the pavement surface and not for the grooves. The groove value, $n_g = 0.010$, was constant for all of the computer runs. Reflex-percussive grooves were not included in these runs because their $n_g$ value is unknown, and because they were not included in the experiments.

## 4.2 EXPERIMENTAL VERSUS ANALYTICAL WATER DEPTHS

Figures 14 through 18 display comparisons of experimental water depths and analytical curves of water depths generated by the modified computer program. Each of the five graphs represents a specific combination of one of the two rainfall intensities with either the ungrooved or the grooved slab at a particular spacing.

Figures 14 and 15 for the ungrooved pavement show three computer model curves, one for each of the three pavement surface n values discussed in Section 3.3.1. The best comparison of data and model appears, surprisingly, to be for n = 0.081, which is the upper limit value from Figure 4 using the average texture of the pavement blemish. It would be difficult to conclude, however, that the blemish controls the hydraulic resistance of the entire slab. Figures 16, 17, and 18 clearly show the reduction of water depths as a result of grooving. In Figure 18 the experimental depths are so small that equation (11) might not be satisfied. Hence, the Manning equation used in the kinematic wave approximation in the computer model may not be valid. This may account for the poor comparison of data and model.

Two types of errors occurred in this study: errors which only affect the measurement of depths and those which affect the comparison of the experimental results with the computer model results. The possible sources of error are defined here, but their magnitudes are uncertain.

Several possibilities exist for depth measurement errors. The flexible tubes that extend to the sensor openings in the slab were sealed to the slab with a commercial windshield sealer compound. The holes are so small that uniformity in sealing was not possible. In some cases, the sealer was rough and bulged up slightly around the top edges of the tubing. The zero water depth datum for each sensor opening is set according to the judgment of the researcher. The effect of capillary action on this setting is uncertain, as is the effect of using a mild detergent as a wetting agent to control this condition by reduction of surface tension. Perhaps a better solution in future studies would be to countersink the sensor openings on the slab prior to placing and sealing the tubing. Another source of error is the possibility

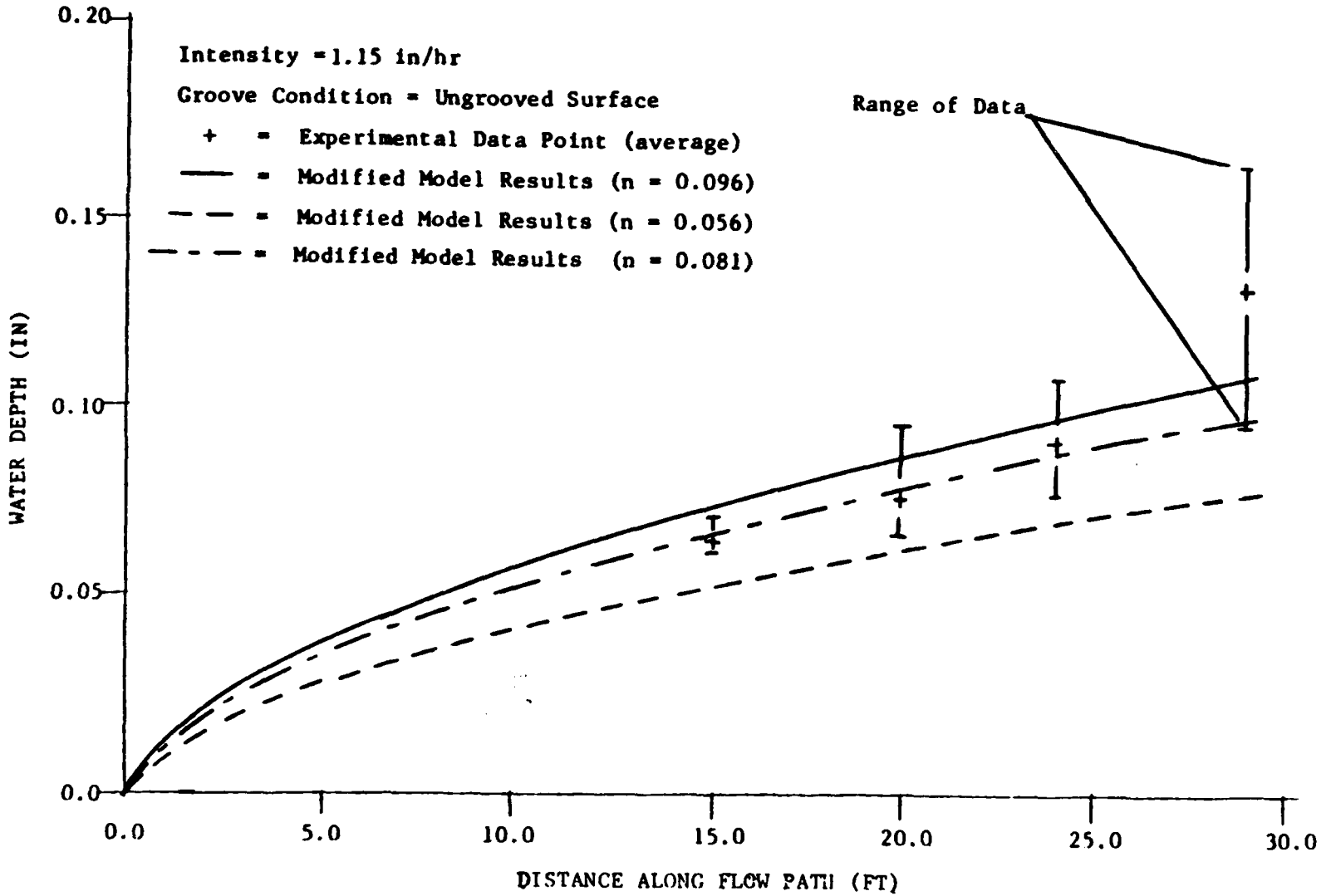


Figure 14. Water Depth versus Distance for Ungrooved Pavement at 1.15 inches per hour

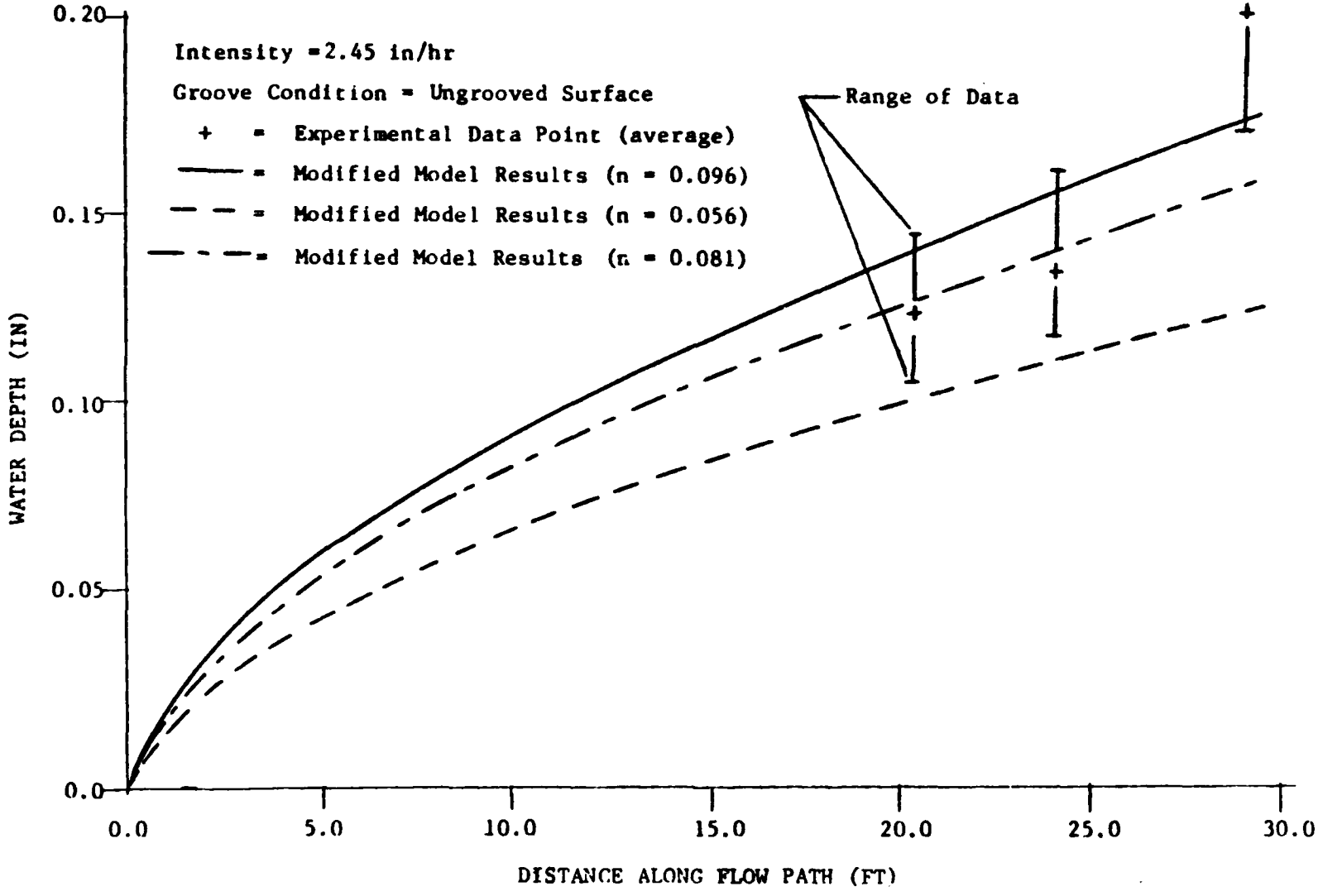


Figure 15. Water Depth versus Distance for Ungrooved Pavement at 2.45 inches per hour

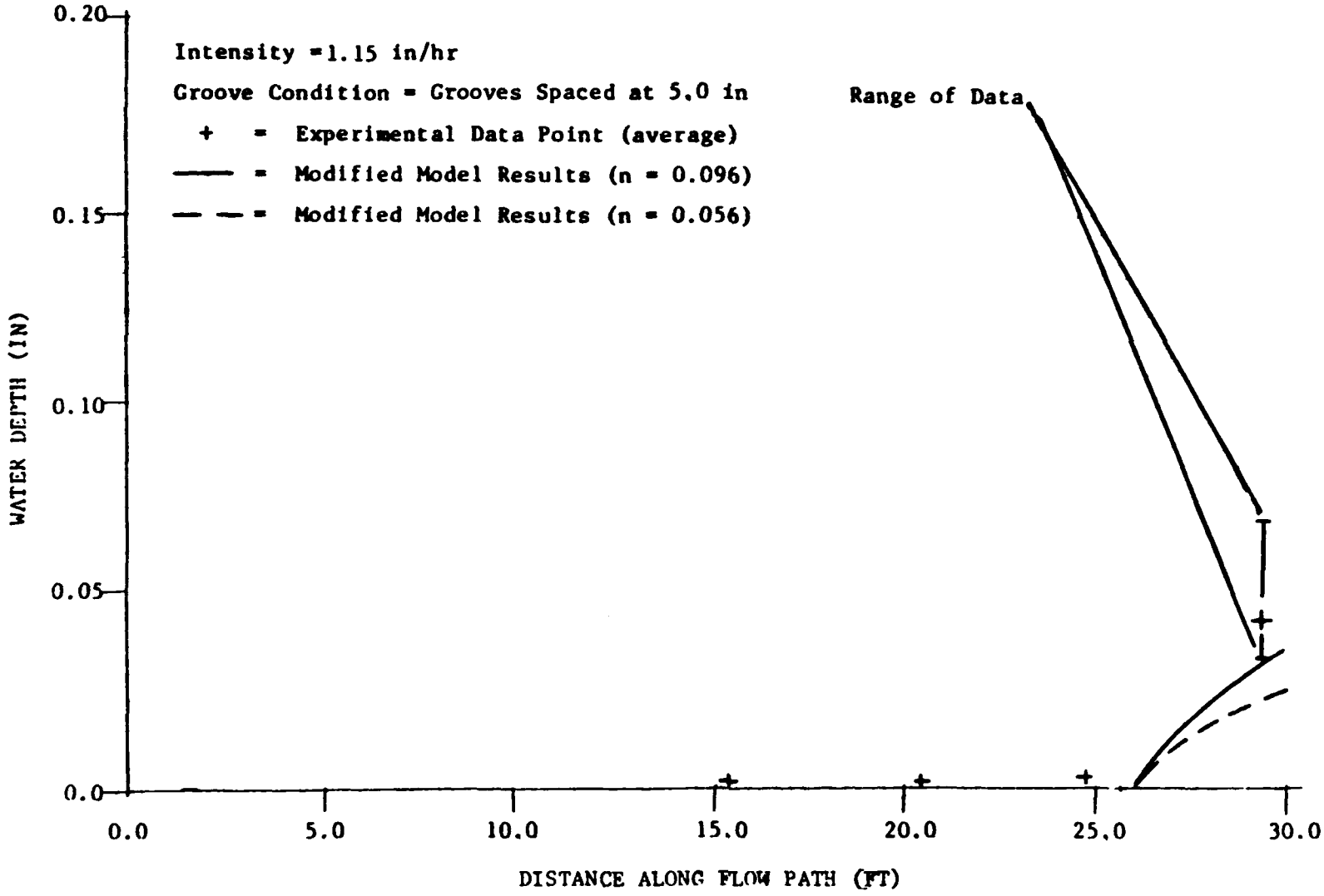


Figure 16. Water Depth versus Distance for 5-in. Rectangular-Groove Spacing at 1.15 inches per hour

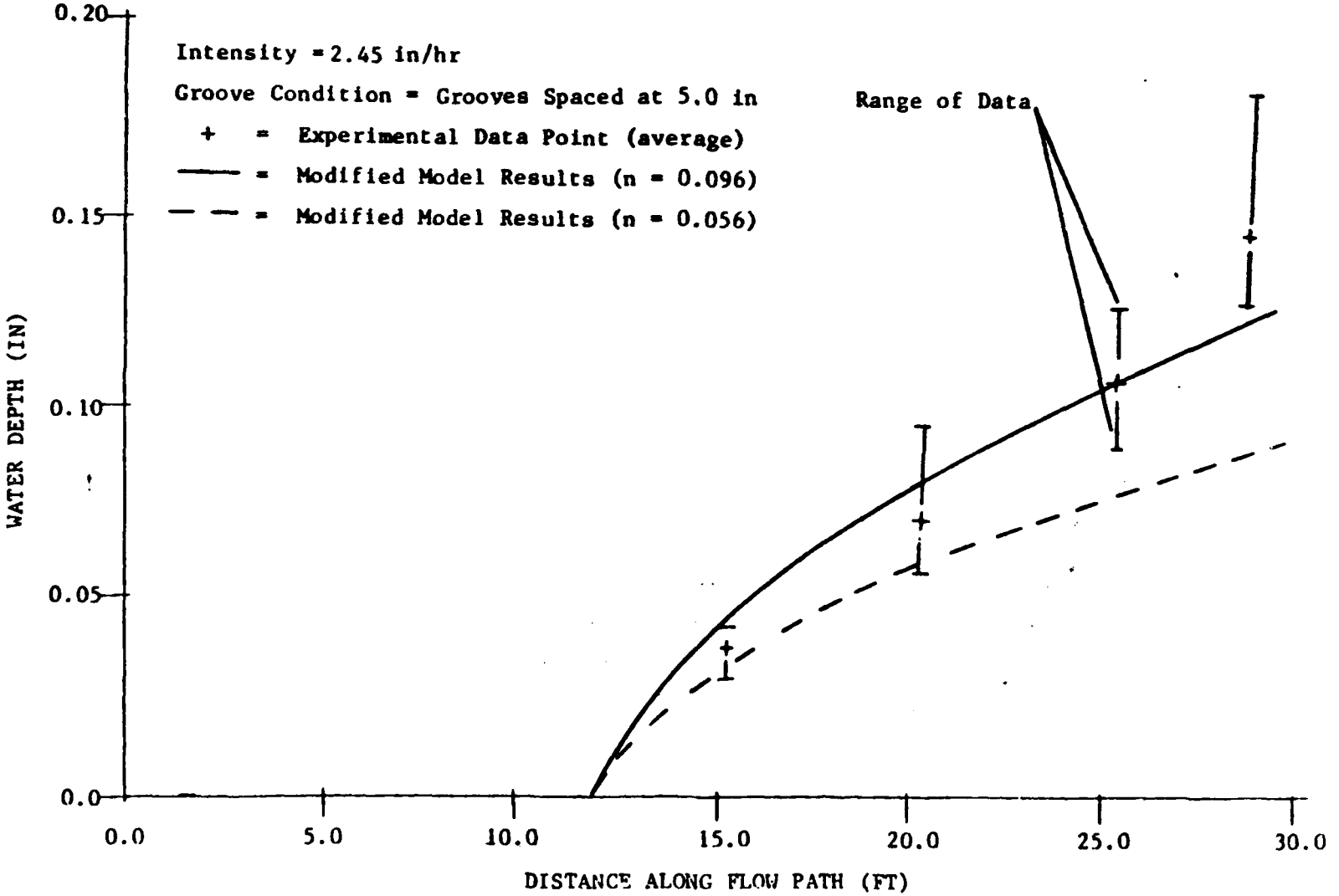


Figure 17. Water Depth versus Distance for 5-in. Rectangular-Groove Spacing at 2.45 inches per hour

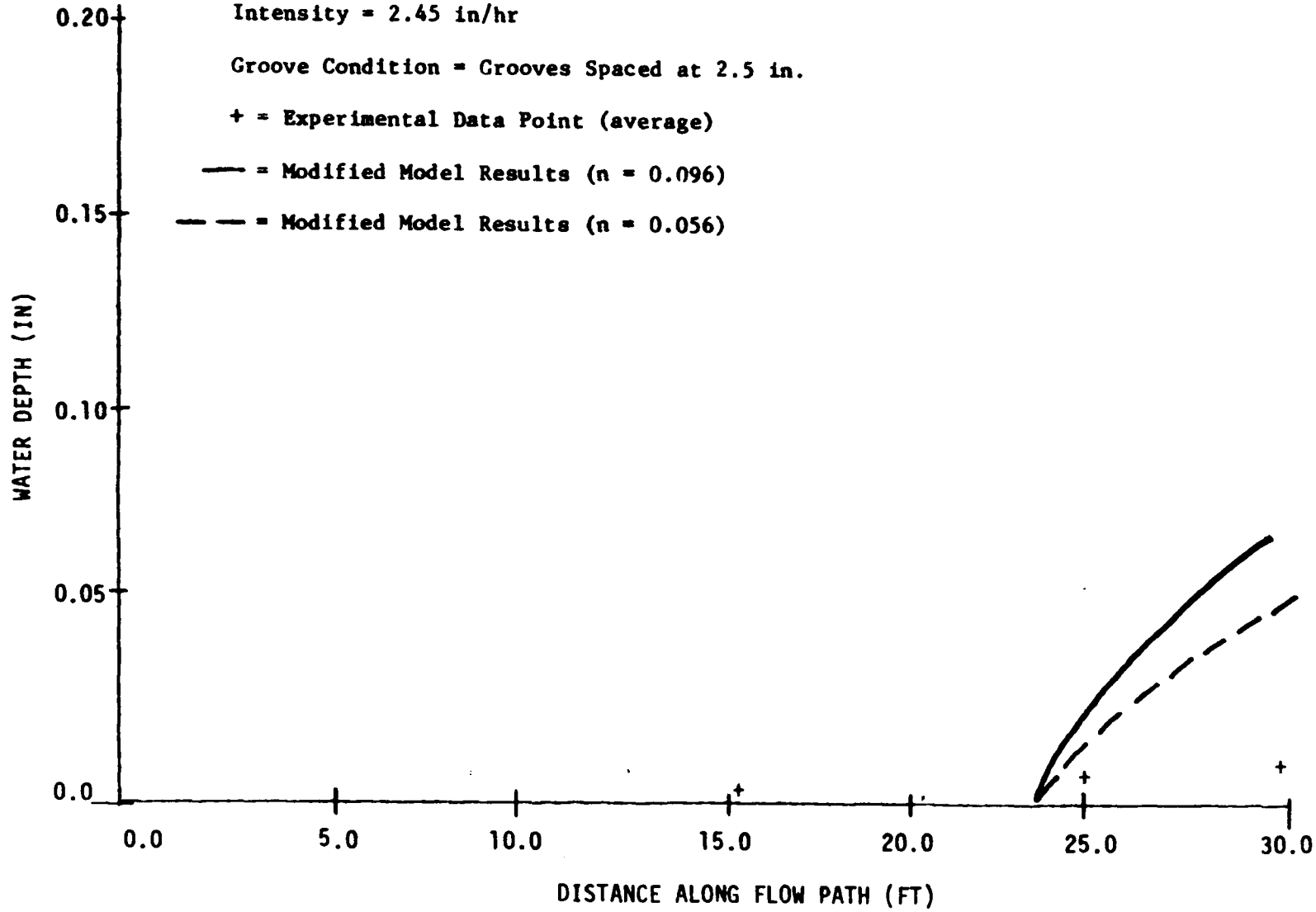


Figure 18. Water Depth versus Distance for 2.5-inch Rectangular-Groove Spacing at 2.45 inches per hour

of air in the tubing, which could cause a false transmission of water depth pressure to a transducer. Since the tubing beneath the slab is not visible, not only is this condition difficult to control, it is difficult even to check. A system where the transducer is located immediately beneath the slab would probably be more reliable. In addition, the calibration of each transducer was accomplished very well, but not exactly to a 100% correlation, to which Figure 12 will attest. Then, too, the fluctuation of voltage readings on the digital multimeter required judgment on the part of the researcher to record a single reading. Such fluctuations in voltage might be augmented according to whether a sensor opening was subject to periodic impact from pelting raindrops or a transducer was kept absolutely dry. Also, in repeated tests the ability to create exactly the same rate and pattern of rainfall by setting the simulator equipment is uncertain. Furthermore, fluctuations in voltage to the pump supplying the rain were never the same from one run to another. If arbitrary values are given to the sources of errors, it is estimated that any depth measurement could be subject to an error of perhaps ±0.04 in.

In comparing the model results with the measured water depths, differences between what the computer assumes in its solution and what actually occurs in the experimental system become sources of error. The computer model assumes an absolutely perfect plane sloping at 1.5% with texture depth, Manning's n, and rainfall intensity perfectly uniform. The slab was constructed within forms set accurately to 1.5% slope. The surface finishing of the concrete was accomplished as carefully as cost would permit, but some slight ponding was evident during tests. The blemish is the primary example of the texture not being uniform. Also, the slab may have settled slightly since construction, perhaps nonuniformly, since a small tension crack is visible on the surface. The rainfall simulation equipment does not generate absolutely uniform rainfall rates: there are spatial variations in rainfall intensities. In the development of the equipment these variations were minimized. Still, standard deviations of the spatial average intensities in this study may be of the order of ±0.3 in./hr. The spatial variations would affect not only the depths down the slab, but also the lateral average depths shown in the Appendix B data. Certainly the experimental errors in measuring depths also affect the comparison.

It does not seem logical to absorb all the errors of experimentation into an adjusted value of Manning's n, but numerous other studies have done so. The question is whether an n value can be accurately predicted for a given situation, or whether it must be measured.

## 4.3 PREDICTION OF WATER DEPTHS FOR RUNWAY LANES

The modified computer program was used to predict equilibrium water depths for rectangular grooves at the four spacings out to a width of runway lane of 100 ft. To justify the selection of a Manning's n value for these computer runs, the upper limit from Figure 4 was used with an average texture depth of 0.026 in. to obtain n = 0.056. The rainfall rate selected was 3 in./hr, the next highest integer value beyond the maximum used in the experiments and near the maximum achievable by the rain simulator. The output for these computer runs is shown in Appendix F. The runs are summarized graphically in Figure 19.

It appears on the graph in Figure 19, and can be shown by equations, that there is an inverse linear relation between spacing and the value at which each curve intersects the distance axis (the predicted point where grooves fill and overflow). If the distance coordinate were multiplied by the spacing, the curves would collapse into one. This has not been done since it was judged that the relation among the variables is clearer as depicted. It should be noted that, on the Appendix F output sheets, equilibrium time at the 100-ft edge is the same for all four grooving conditions. This assumption is reasonable since the equilibrium flow rate off the edge of the pavement or at any other given distance downstream must be the same for all four cases at 3.00 in./hr. The principle of conservation of mass would be true for any hydraulic roughness as well, although hydraulic roughness was not varied for the four cases. The following calculation will illustrate that total flow off the edge of the runway must be equal to total flow onto the runway at equilibrium conditions:

$$\begin{aligned}\text{Flow onto pavement} &= 3 \text{ in./hr} \times 1 \text{ ft}/12 \text{ in.} \times 1 \text{ hr}/3600 \text{ sec} \\ &\quad \times 100 \text{ ft} \times 15 \text{ ft} \\ &= 0.104 \text{ cfs}\end{aligned}$$

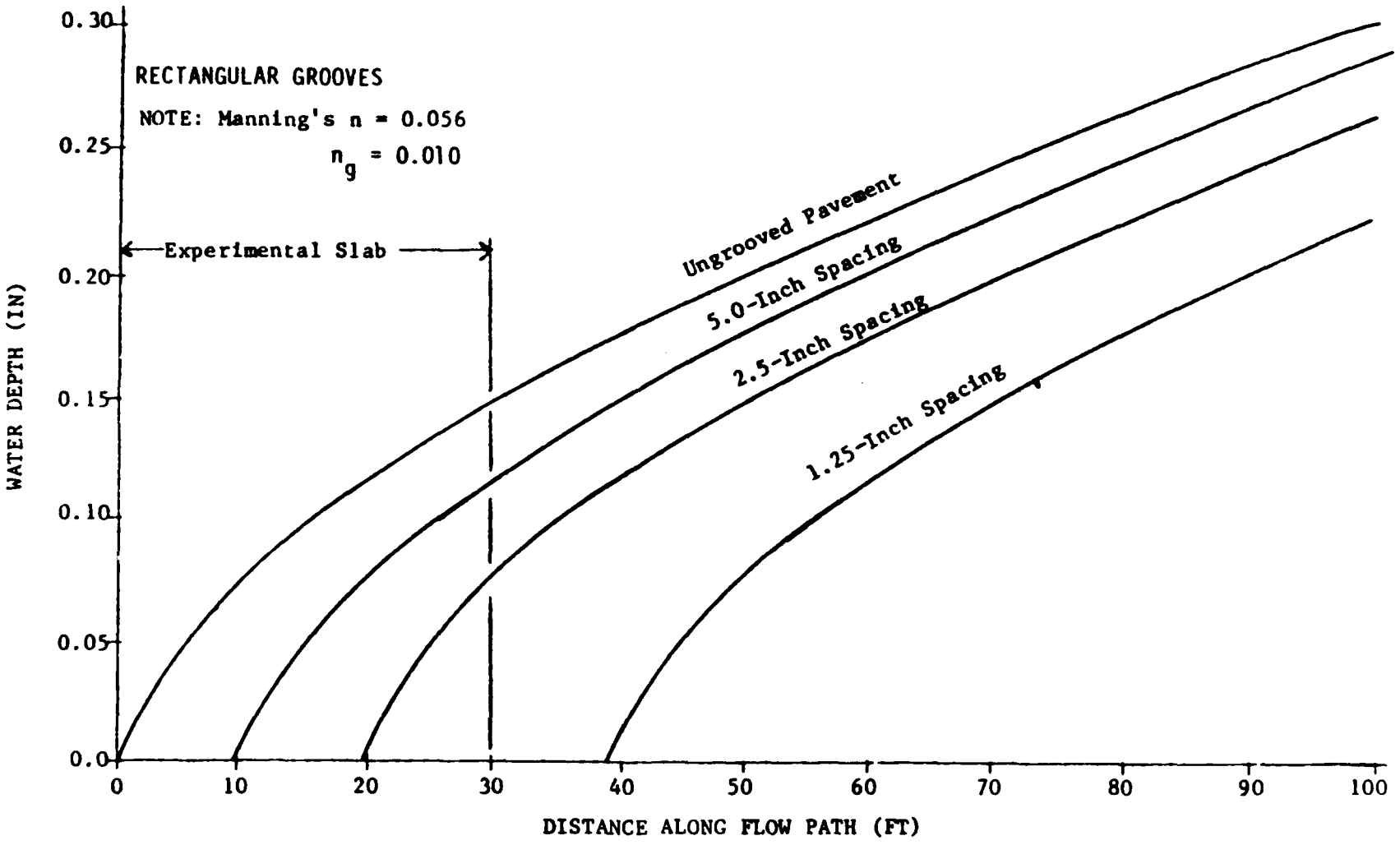


Figure 19. Predicted Water Depths for Various Rectangular-Groove Spacings at 3.00 inches per hour

A check of the Appendix F output will confirm that this figure agrees with the flow off the edge of the runway as calculated from pavement roughness and grooving considerations by using equation (10).

From Figure 19, it can be observed that the predicted maximum reduction in water depths due to grooving is about 0.18 in. for rectangular grooves spaced at 1.25 in. at a distance of about 39 ft. The same point is shown on Figure 20 as a 100% reduction in depth. The curves of Figure 20 also collapse into a single curve in a manner similar to those in Figure 19.

Figure 21 represents curves of prediction of water depths for the reflex-percussive grooves of Figure 1 at the same surface roughness (0.056) and rainfall intensity (3.00 in./hr) as for the rectangular grooves in Figure 19. However, the groove roughness ($n_g$) is uncertain for these grooves. The points necessary to plot these curves were computed manually, since no provision was made for this shape in the modified computer program. It appears that at the same $n_g$ value of 0.010, these grooves are much more efficient in reducing water depths than are rectangular grooves spaced at 2.5 in., and almost as efficient as rectangular grooves spaced at 1.25 in.

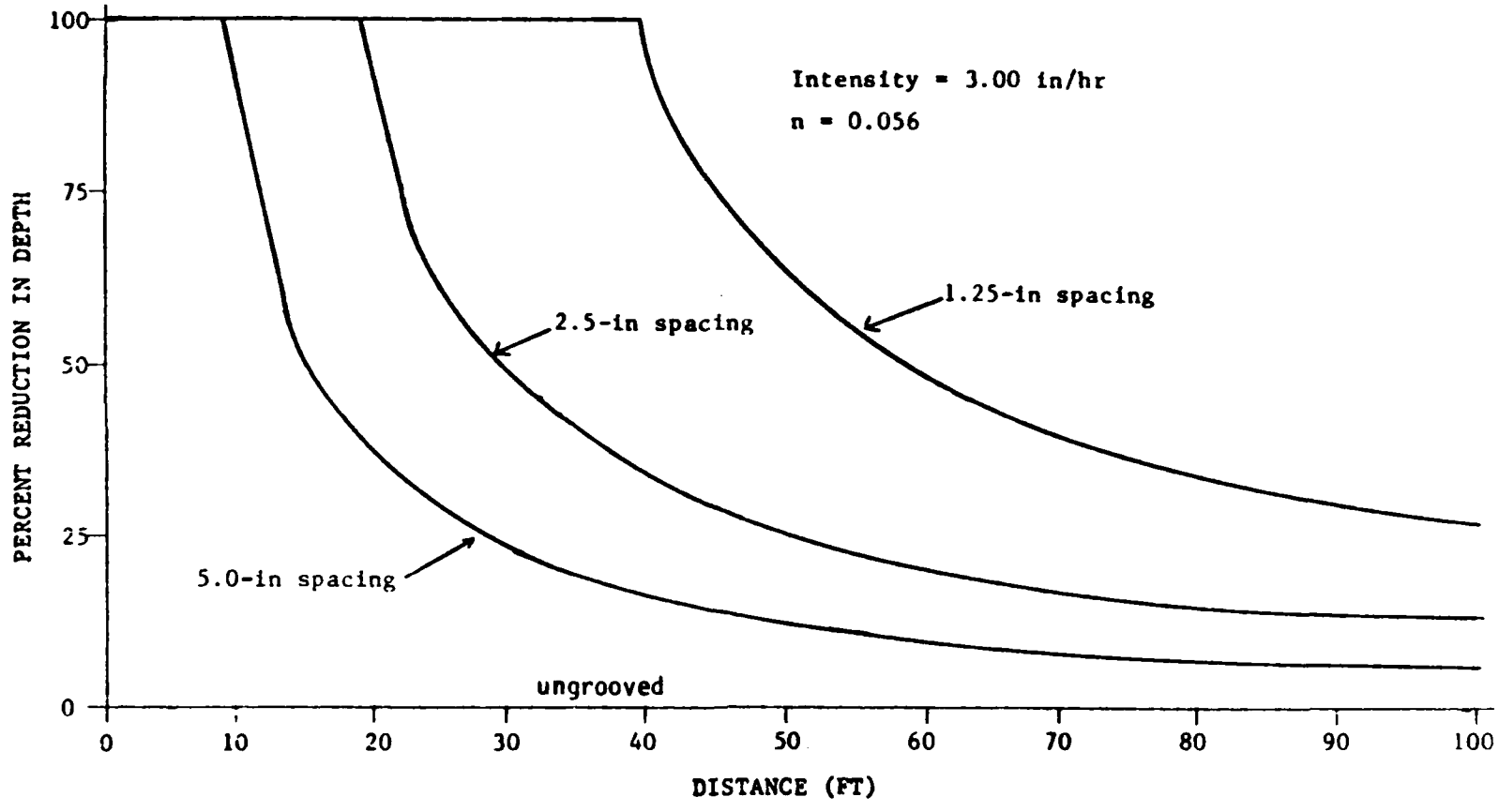


Figure 20. Predicted Percent Reduction in Depth versus Distance for Various Rectangular-Groove Spacings at 3.00 inches per hour

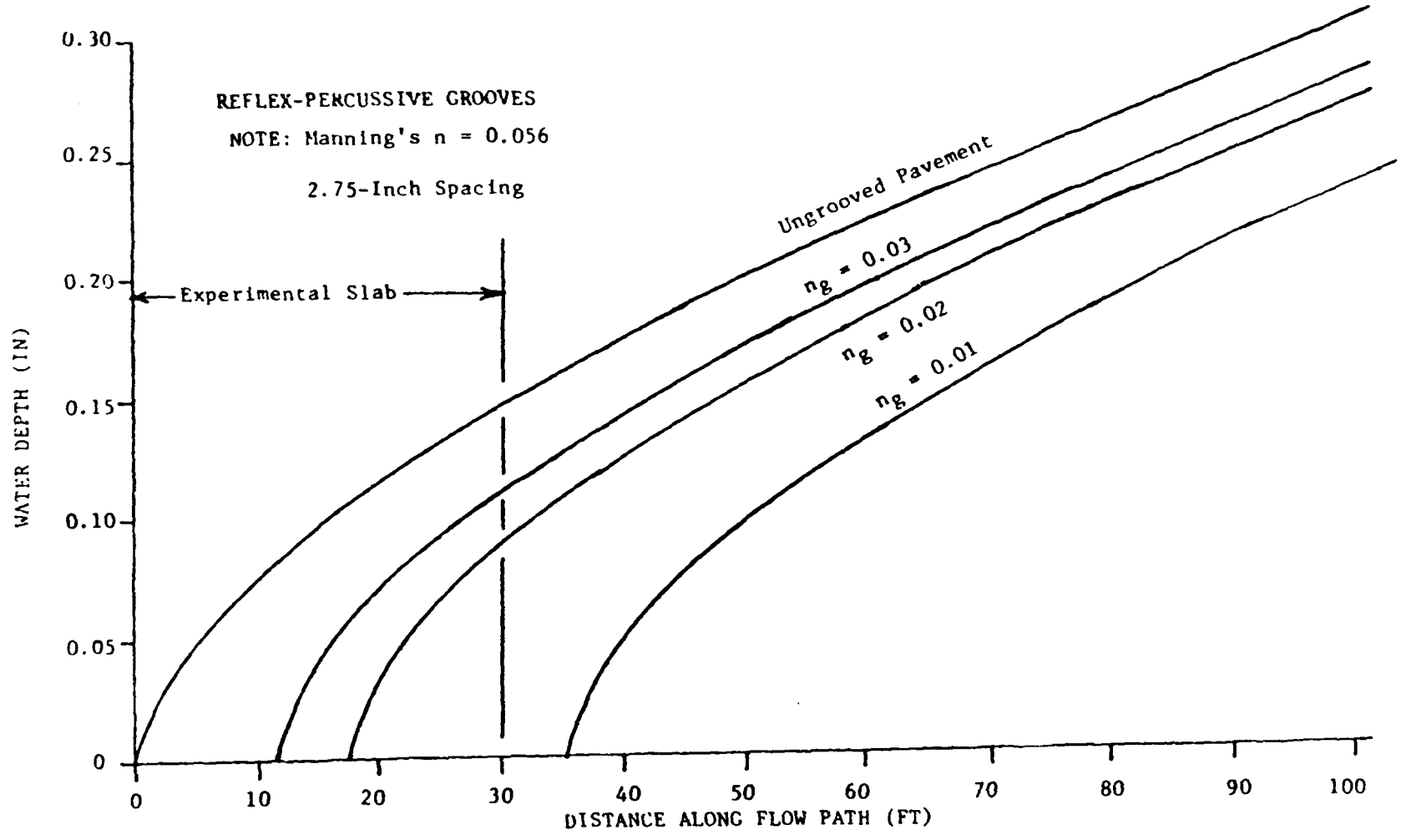


Figure 21. Predicted Water Depths for Reflex-Percussive Grooves at 3.00 inches per hour

# 5. SUMMARY

The subject of this study has been the prediction of runoff characteristics from a laterally grooved runway during a steady, uniform rainfall. The conclusions and recommendations will address this situation. However, the authors believe that one of the principal advantages of grooving is the quick draining of the pavement after rain has stopped, a point also made by Horne [26].

## 5.1 CONCLUSIONS

1. The kinematic wave approximation to the shallow water equations, together with an estimate of hydraulic roughness (Manning's n), is a reasonable model for predicting runoff characteristics from a grooved or ungrooved runway.

2. The lateral grooving of runways enhances drainage in the form of decreased water depths. The following table gives a quantitative indication of the decreases predicted from Figures 19 and 20 for 3.00 inches of rain per hour and n = 0.056.

| Groove Spacing (in.) | 100% Reduction in Water Depth through L (ft) | Maximum Reduction in Water Depth (in.) | % Reduction in Water Depth at L = 100 ft |
|---|---|---|---|
| 1.25 | 39 | 0.18 | 27 |
| 2.50 | 19 | 0.11 | 14 |
| 5.00 | 9 | 0.07 | 7 |

3. The efficiency of a groove shape in reducing water depths is directly dependent on its volumetric capacity and inversely dependent on its hydraulic roughness coefficient (Manning's n).

4. The topography of a runway surface subject to steady, uniform rain will determine the magnitude of equilibrium runoff depths that will occur there; however, it will not determine the magnitude of equilibrium runoff flow rates, which must obey the law of conservation of mass.

## 5.2 RECOMMENDATIONS

A logical continuation of this research would be to repeat the experimental analyses for an asphaltic concrete surface (probably a wearing course) laid over the existing portland cement concrete slab. The effects of an adverse wind, and possibly a variable rainfall rate, on the pavement drainage should also be studied. By retaining the groove shape as rectangular, a commonly occurring field condition would be simulated. Such a study might be conducted in 12 to 15 months. Looking even further ahead, the same runoff tests should be conducted for asphaltic concrete surfaces with reflex-percussive grooves. Depending on what parameters are chosen, a study of this nature might be completed in an additional 12 months.

Also, additional experimental and/or theoretical work should be performed as follows:

1. With reflex-percussive grooves, particularly with regard to their hydraulic roughness;

2. To refine further the notion of hydraulic roughness versus macrotexture, as depicted in Figure 4, by carefully controlled channel experiments with typical runway pavement surfaces;

3. On the effects of ponding on runways, which may be more crucial than runoff depths from the standpoint of hydroplaning (the technology to determine accurate runway topography would have to be developed to detect the slightest rutting, and perhaps a two-dimensional runoff model could be developed);

4. On how the flow occurs over grooves once they are filled. This research assumed a planar flow over the filled grooves at an n equal to that of the pavement surface.

## REFERENCES


1. Agrawal, S. K. and Daiutolo, H. The Braking Performance of an Aircraft Tire on Grooved Portland Cement Concrete Surfaces. Interim Report. Report No. FAA-RD-80-78. Federal Aviation Administration, Washington, D.C., January 1981.

2. Horne, Walter B. and Dreher, R. C. Phenomena of Pneumatic Tire Hydroplaning. Report No. NASA-TND-2056. National Aeronautics and Space Administration, Hampton, Va., 1963.

3. Reed, J. R., Kibler, D. F., and Proctor, M. L. Analytical Model of Grooved Pavement Runoff. Interim Report for Phase I, submitted to Federal Aviation Administration, Contract No. DTFA01-81-C-10037. PTI Report 8206. Pennsylvania Transportation Institute, The Pennsylvania State University, March 1982, rev. July 1982.

4. Reed, J. R., Kibler, D. F., and Agrawal, S. K. "Mathematical Model of Grooved Pavement Runoff." Paper presented (publication pending) at the 62nd Annual Meeting of the Transportation Research Board, Washington, D.C., January 1983.

5. Reed, J. R., Kibler, D. F., and Proctor, M. L. Experimental Study of Grooved Pavement Runoff. Interim Report for Phase II, submitted to Federal Aviation Administration, Contract No. DTFA01-81-C-10037. PTI Report 8226. Pennsylvania Transportation Institute, Pennsylvania State University, December 1982.

6. Agrawal, S. K. Braking of an Aircraft Tire on Grooved and Porous Asphaltic Concrete. Final Report. Report No. FAA-RD-82/77, FAA-CT-82/147, Federal Aviation Administration Technical Center, Atlantic City Airport, N.J., January 1983.

7. Henderson, F. M. Open Channel Flow. Macmillan, New York, 1966.

8. Chow, V. T. Open-Channel Hydraulics. McGraw-Hill, New York, 1959.

9. Liggett, J. A. and Woolhiser, D. A. "Difference Solutions of the Shallow-Water Equation." Journal of the Engineering Mechanics Division (ASCE), Vol. 93, EM2, April 1967, pp. 39-71.

10. Lighthill, M. J. and Whitham, C. B. "On Kinematic Waves I: Flood Movement in Long Rivers." Proceedings, Royal Society of London, Series A, Vol. 229, 1955.

11. Woolhiser, D. A. and Liggett, J. A. "One-Dimensional Flow Over a Plane--the Rising Hydrograph." Water Resources Research, Vol. 3, No. 3, September 1967, pp. 753-771.

12. Kibler, D. F. and Aron, G. "Effects of Parameter Sensitivity and Model Structure in Urban Runoff Simulation." Proceedings, International Symposium on Urban Storm Water Management. University of Kentucky, Lexington, Ky., July 1978.

13. Izzard, C. F. "Hydraulics of Runoff from Developed Surfaces." Proceedings, Highway Research Board, Vol. 26, 1946, pp. 129-146.

14. Gallaway, B. M., Schiller, R. W., and Rose, J. G. The Effects of Rainfall Intensity, Pavement Cross Slope, Surface Texture, and Drainage Length on Pavement Water Depths. Research Report 138-5. Texas Transportation Institute, Texas A&M University, College Station, Texas, May 1971.

15. Reed, J. R. and Kibler, D. F. "Hydraulic Resistance of Pavement Surfaces." Journal of Transportation Engineering, Vol. 109, No. 2, March 1983, pp. 286-296.

16. Ross, N. F. and Russam, K. The Depth of Rain Water on Road Surfaces. RRL Report LR 236. Road Research Laboratory, Crowthorne, Berks., U.K., 1968.

17. Kibler, D. F., Aron, G., Riley, K. A., Osei-Kwadwo, G., and White, E. L. Recommended Hydrologic Procedures for Computing Urban Runoff from Small Watersheds in Pennsylvania. Institute for Research on Land and Water Resources, The Pennsylvania State University, University Park, Pa., February 1982.

18. Rose, J. G. et al. "Summary and Analysis of the Attributes of Methods of Surface Texture Measurement." Special Technical Publication 53. American Society for Testing and Materials, Philadelphia, June 1972.

19. Henry, J. J. and Hegmon, R. R. "Pavement Texture Measurement and Evaluation." ASTM Special Technical Publication 583. Philadelphia 1975, pp. 3-17.

20. U.S. Army Corps of Engineers. Data Report, Airfield Drainage Investigations. Los Angeles District, Office of the Chief of Engineers, Airfields Branch, Military Construction, October 1954.

21. Morris, E. M. and Woolhiser, D. A. "Unsteady One-Dimensional Flow Over a Plane: Partial Equilibrium and Recession Hydrographs." Water Resources Research, Vol. 16, No. 2, April 1980, pp. 355-360.

22. Rovey, E. W., Woolhiser, D. A., and Smith, R. E. "A Distributed Kinematic Model of Upland Watersheds." Hydrology Paper No. 93. Colorado State University, Fort Collins, 1977.

23. Chen, C. L. "Generalized Manning Formula for Urban Storm Runoff Routing." Second International Conference on Urban Storm Drainage. University of Illinois, Champaign-Urbana, June 1981.

24. Davis, D. G. "The Development of a System for the Physical Simulation of Rainfall on Highway Pavements." Report in Civil Engineering. The Pennsylvania State University, University Park, Pa., November 1982.

25. U.S. Army Corps of Engineers, HEC-1 Flood Hydrograph Package, Users Manual. Hydrologic Engineering Center, Davis, Calif., September 1981.

26. Horne, W. B. "Safety Grooving, Hydroplaning, and Friction." Listed as New Technical Report in International Groover, International Grooving and Grinding Association, New York, 1981.

## APPENDIX A. TECHNICAL DATA ON PRESSURE TRANSDUCERS

MANUFACTURER: Foxboro/ICT Inc., San Jose, California

DESCRIPTION: Series 1813-003-1

A linear integrated circuit transducer which senses pressure by means of a wheatstone bridge diffused into a silicon diaphragm. The output signal is linear and proportional to the applied pressure.

PRESSURE RANGE: 0 to 10 in. of $H_2O$, gage

INPUT SIGNAL: 1.5 mA (DC)

OUTPUT SIGNAL: 15 mV ± 5 mV

ZERO READING: 0 ± 5 mV

RESPONSE EQUATION: $Y = K (\Delta V)$

where

$Y$ = change in pressure head (in. of $H_2O$)
$\Delta V$ = change in voltage (mV)
$K$ = calibration coefficient, individual for each transducer (in./mV)

CALIBRATION COEFFICIENTS (K) (also see Figure 6):

| TRANSDUCER | (K) |
|---|---|
| 1 | 0.056 |
| 2 | 0.063 |
| 3 | 0.063 |
| 4 | 0.068 |
| 5 | 0.074 |
| 6 | 0.074 |
| 7 | 0.083 |
| 8 | 0.083 |
| 9 | 0.090 |
| 10 | 0.094 |

## APPENDIX B. EQUILIBRIUM WATER DEPTH DATA

Table B-1. Average Water Depths (in.) at a Rainfall Intensity of 1.15 in./hr on an Ungrooved Surface

| Distance (ft) | Location A | B | C | D | Lateral Average |
|---|---|---|---|---|---|
| 15.6 (Range) | --* | 0.068<br>0.064-0.075 | -- | -- | 0.068 |
| 20.7 | 0.082<br>0.070-0.098 | -- | 0.079<br>0.071-0.095 | -- | 0.080 |
| 24.8 | 0.093<br>0.085-0.104 | 0.108<br>0.097-0.112 | 0.088<br>0.080-0.099 | -- | 0.095 |
| 29.5 | 0.169<br>0.142-0.212 | 0.118<br>0.097-0.128 | -- | 0.121<br>0.115-0.142 | 0.136 |

* Blanks indicate data not taken or unreliable readings.

Table B-2. Average Water Depths (in.) at a Rainfall Intensity of 2.45 in./hr on an Ungrooved Surface

| Distance (ft) | Location A | B | C | D | Lateral Average |
|---|---|---|---|---|---|
| 15.6 (Range) | -- | -- | -- | -- | -- |
| 20.7 | 0.132<br>0.112-0.147 | -- | 0.118<br>0.109-0.133 | -- | 0.125 |
| 24.8 | 0.142<br>0.122-0.155 | -- | 0.152<br>0.120-0.164 | -- | 0.147 |
| 29.5 | 0.281<br>0.223-0.302 | 0.191<br>0.180-0.229 | -- | 0.185<br>0.174-0.208 | 0.212 |

Table B-3. Average Water Depths (in.) at a Rainfall Intensity of 1.15 in./hr on a Grooved Surface with 5-in. Spacing

| Distance (ft) | Location A | B | C | D | Lateral Average |
|---|---|---|---|---|---|
| 15.6 (Range) | -- | 0.000 | -- | -- | -- |
| 20.7 | 0.000 | 0.000 | 0.000 | -- | 0.000 |
| 24.8 | 0.000 | -- | 0.000 | -- | 0.000 |
| 29.5 | 0.052<br>0.048-0.069 | 0.039<br>0.033-0.058 | -- | -- | 0.046 |

Table B-4. Average Water Depths (in.) at a Rainfall Intensity of 2.45 in./hr. on a Grooved Surface with 5-in. Spacing

| Distance (ft) | Location A | B | C | D | Lateral Average |
|---|---|---|---|---|---|
| 15.6 (Range) | -- | 0.040<br>0.031-0.045 | -- | -- | 0.040 |
| 20.7 | 0.075<br>0.060-0.081 | 0.071<br>0.053-0.097 | -- | -- | 0.073 |
| 24.8 | 0.118<br>0.103-0.128 | 0.109<br>0.092-0.125 | 0.102<br>0.095-0.113 | -- | 0.110 |
| 29.5 | 0.159<br>0.131-0.187 | 0.142<br>0.131-0.158 | -- | 0.138<br>0.129-0.155 | 0.146 |

Table B-5. Average Water Depths (in.) at a Rainfall Intensity of 2.45 in./hr. on a Grooved Surface with 2.5-in. Spacing

| Distance (ft) | Location A | B | C | D | Lateral Average |
|---|---|---|---|---|---|
| 15.6 (Range) | -- | -- | -- | -- | -- |
| 20.7 | 0.000 | 0.000 | 0.000 | 0.000 | 0.000 |
| 24.8 | 0.003<br>0.001-0.004 | 0.002<br>0.001-0.004 | 0.000 | 0.000 | 0.003 |
| 29.5 | 0.007<br>0.005-0.009 | 0.005<br>0.003-0.007 | 0.000 | 0.002<br>0.001-0.002 | 0.004 |

# APPENDIX C. FLOW CHART FOR MODIFIED COMPUTER PROGRAM

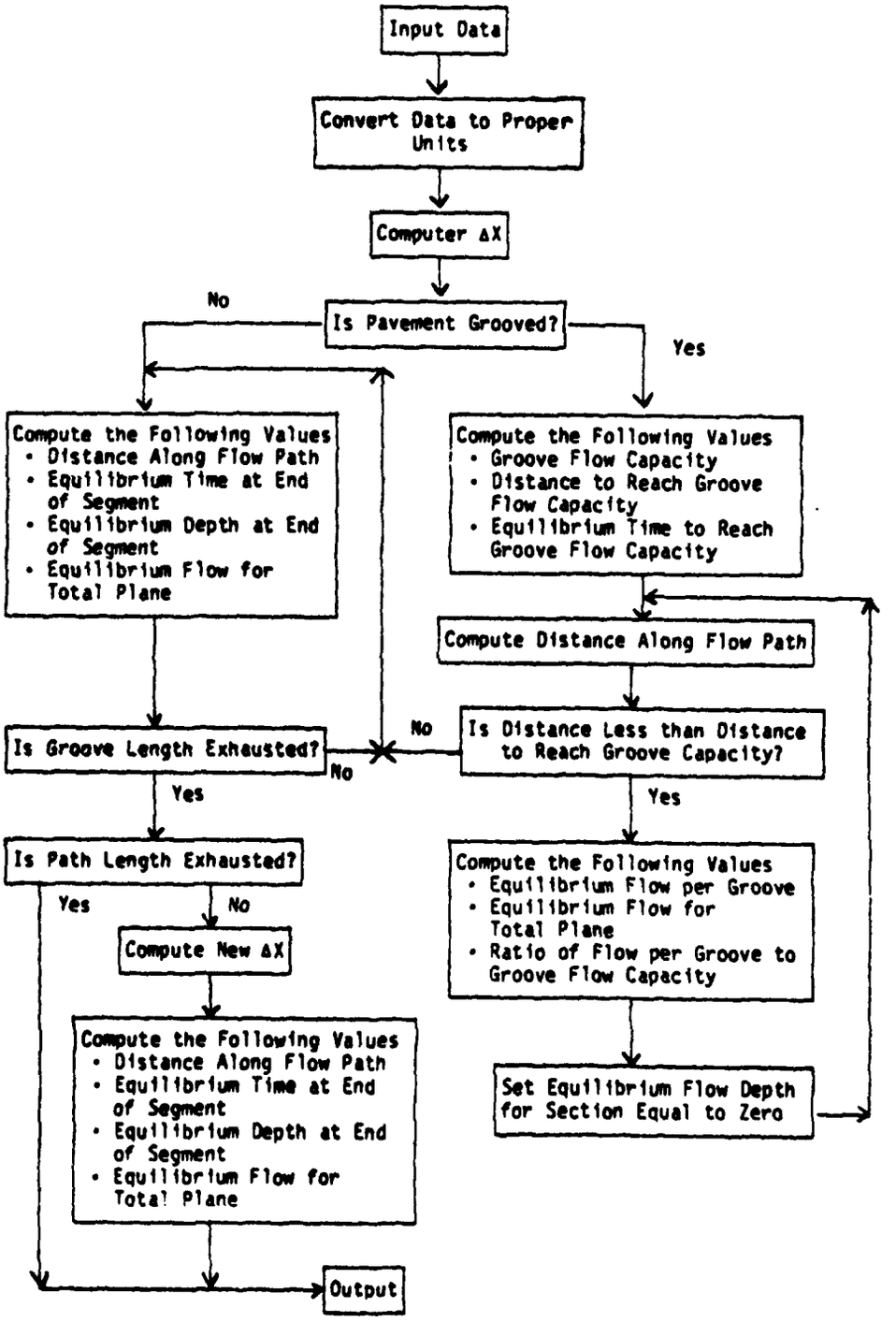

# APPENDIX D. LISTING OF MODIFIED COMPUTER PROGRAM IN FORTRAN IV

```
*** FSO-WATFIV *** 20-0 (03/08/81--1844)

                C   THIS PROGRAM IS DESIGNED TO PREDICT WATER DEPTHS ON A PLANE SURFACE.
                C  VARIABLES INCLUDE SURFACE TEXTURE, SLOPE, RAINFALL INTENSITY AND
                C  MANNINGS ROUGHNESS.  ALLOWANCE IS MADE FOR UNGROOVED PAVEMENT OR
                C  RECTANGULAR GROOVES.  THE GROOVES CAN BE OF ANY SIZE, SPACING OR
                C  LENGTH.
                C
      1              REAL TEQ(200),YPLANE(200),YINCH(200),QPL(200),DIST(
                    $200),QTOT(200), FLOWR(200),GRATIO(200)
      2              READ, J
      3              DO 101 K = 1,J,1
      4              PRINT 160,K
      5           160 FORMAT ('1',I2)
      6              PRINT, ' '
      7               PRINT,'
                    SAM OUTPUT'
      8               PRINT, '
                    UNIVERSITY'
      9               PRINT, '
                    OF ILLINOIS'
     10               PRINT, '
                C
                C
     11              READ, TD,ROUGHF,ROUGHG
     12              READ, RF
     13              READ, SLOPE
     14              READ, ISHAPE,GDEPTH,GWIDTH,GSPACE
     15              READ, PLENG,GLENG,WIDTH
                C
                C
     16              IF (ISHAPE .EQ. 0) PRINT, '  UNGROOVED SURFACE'
     17              IF (ISHAPE .EQ. 1) PRINT, '  RECTANGULAR GROOVES'
     18              PRINT,' '
                C
                C    CONVERSION OF INPUT DATA TO FOOT-SECOND UNITS
                C
     19              QRF = RF/43200
     20              SPACE = GSPACE/12
     21              GRW = GWIDTH/12
     22              GRD = GDEPTH/12
     23              DELTAX = GLENG/100
     24              ALPHA =(1.49/ROUGHF)*(SLOPE)**(0.5)
                C
                C   GROOVE CONFIGURATION DETERMINATION
                C
     25              IF (ISHAPE .EQ. 1) GO TO 10
                C
                C     DEPTH CALCULATIONS UNGROOVED CASE
                C
     26              DO 102 I =1,100,1
     27                 TEQ(I) = 1/QRF*(DELTAX * I * QRF/ALPHA)**(3.60)
     28                 YPLANE(I) = QRF*TEQ(I)
     29                 QPL(I) = ALPHA * ((YPLANE(I))**(1.667))*SPACE
     30                 YINCH(I) = YPLANE(I) *12
     31                 QTOT(I) = QPL(I) * (WIDTH/SPACE)
     32                 DIST(7) = DELTAX* I
     33           102 CONTINUE
     34              GO TO 60
                C
```

```
C      DEPTH CALCULATIONS GROOVED CASE
C
35     10  FLOWG=1.49/ROUGHG*GRD*GRS*(GRS*GRD/(GRW+2*GRD))**(0.667)*
          ESLOPE**(0.5)
36          GO TO 30
37      25     PRINT, 'INVALID SHAPE PARAMETER    '
38             GO TO 777
39      30  IF (ISHAPE .NE. 0) GRENO=FLOWG/(QRF*SPACE)
40          I = 1
41      40  IF ((DELTAX*I) .LE.  GRENO) THEN DO
42              TEQ(I)=1/QRF*(DELTAX*I*QRF/ALPHA)**(0.60)
43              QPL(I)=ALPHA*(QRF*TEQ(I))**(1.6667)*SPACE
44              GRATIO(I) = QPL(I)/FLOWG
45              YINCH(I)=0.0
46              DIST(I) = DELTAX * I
47              QTOT(I) =QPL(I)*WIDTH/SPACE
48              I = I+1
49              GO TO 40
50          ELSE DO
51              TEQGR=1/QRF*(GRENO*QRF/ALPHA)**(0.60)
52              L=I
53          DSTEP = DELTAX *(L) - GRENO
54          END IF
55          DO 65 I = L,100,1
56               TEQ(I) =  1/QRF*((DELTAX*I-GRENO)*QRF/ALPHA)**(0.60)
57               YPLANE(I) = QRF*TEQ(I)
58               YINCH(I) = YPLANE(I) * 12
59               QPL(I) = ALPHA * ((YPLANE(I))**(1.667))*SPACE + FLOWG
60               QTOT(I) = QPL(I)*WIDTH/SPACE
61               DIST(I)=DELTAX*I
62               GRATIO(I)=4.5
63      65  CONTINUE
C
64      60  IF (ISHAPE .EQ. 0) THEN DO
65              DO 99 N=1,200,1
66                  GRATIO(N)=4.5
67      99          CONTINUE
68              TEQGR=0.0
69          ELSE DO
70            N= 0
71          END IF
C
C       DEPTH CALCULATIONS FOR CASE WHERE GROOVES DO NOT RUN
C       ENTIRE PAVEMENT LENGTH
C
72          IF (PLENG .GT. GLENG ) THEN DO
73             YPLANE(100) =(QPL(100) / (ALPHA*SPACE))**(0.6)
74             DX = (PLENG-GLENG)/10.0
75             YINCH (100) = YPLANE(100) * 12
76             DO 50 I = 101,110,1
77                TEQ(I)= 1/QRF*((DX*(I-100)+DELTAX*100)*QRF/ALPHA)**(0.60)
78                YPLANE(I) = QRF*TEQ(I)
79                QPL(I) = ALPHA * ((YPLANE(I))**(1.667))*SPACE
80                YINCH(I) = YPLANE(I) *12
81                QTOT(I) = QPL(I) * (WIDTH/SPACE)
82                GRATIO(I)=4.5
83                DIST(I) = DX*(I-100) + DELTAX*100
84      50     CONTINUE
85             TIMEEQ = 1/QRF*(PLENG*QRF/ALPHA)**(0.60)
86             FLOWEQ = QTOT(110)
```

```
            IEND = 110
          ELSE DO
               TIMEEQ = 1/QRF*(PLENG*QRF/ALPHA)**(0.60)
               FLOWEQ = QTOT(100)
               IEND = 100
          IF (ISHAPE .EQ. 0) GRENO=0.0
          END IF
     C
     C    OUTPUT ROUTINE
     C
          PRINT, '  TEXTURE DEPTH (INCHES):       ',TD
          PRINT, '  MANNINGS "N" FACTOR(SURFACE):',ROUGHP
          PRINT, '  MANNINGS "N" FACTOR(GROOVES):',ROUGHG
          PRINT, '  RAINFALL INTENSITY (IN/HR):  ', RF
          PRINT, '  RUNWAY SLOPE (FT/FT) :       ', SLOPE
          PRINT, ' '
          PRINT, '  GROOVE SPACING (IN): ', GSPACE
          PRINT, '  GROOVE DEPTH (IN):   ', GDEPTH
          PRINT, '  GROOVE WIDTH (IN):   ', GWIDTH
          PRINT, ' '
          PRINT, '  SURFACE LENGTH (FT) :', PLENG
          IF (ISHAPE .EQ. 2) GLENG=0.0
          PRINT, '  GROOVE LENGTH (FT) : ' , GLENG
          PRINT, '  SURFACE WIDTH (FT) :', WIDTH
          PRINT, ' '
     C
          PRINT, '  TOTAL FLOW AT END OF PLANE(CFS) : ', FLOWEQ
          PRINT, '  TOTAL EQUILIBRIUM FLOW TIME (SEC): ', TIMEEQ
          PRINT, '  GROOVE EQUILIBRIUM LENGTH (FT):   ',GRENO
          PRINT, ' '
          PRINT, ' '
          PRINT, '        SEGMENT       DISTANCE(FT)          FILM DEPTH(IN)
     $     FLOW(CFS/SPACING)       TOTAL FLOW(CFS)   GROOVE FLOW RATIO'
          PRINT, ' '
          DO 203 I=1,9,1
          PRINT, I, DIST(I), YINCH(I), QPL(I), QTOT(I), GRATIO(I)
     203  CONTINUE
          DO 204 I=10,IEND,5
            PRINT,I, DIST(I), YINCH(I), QPL(I), QTOT(I) , GRATIO(I)
     204  CONTINUE
          GO TO 777
     777  N = 0
     101  CONTINUE
          STOP
          END
**WARNING**  UNREFERENCED STATEMENT     25 USED IN LINE     37 FOLLOWS A TRANSFER

STATEMENTS EXECUTED=    4043

CORE USAGE       OBJECT CODE=    6720 BYTES,ARRAY AREA=    6400 BYTES,TOTAL AREA AVAILABLE=  190464  BYTES

DIAGNOSTICS        NUMBER OF ERRORS=       0, NUMBER OF WARNINGS=       1, NUMBER OF EXTENSIONS=       3

,COMPILE TIME=     0.07 SEC,EXECUTION TIME=     0.10 SEC,                                                    WATFIV - MAR 1980 V2L0
```

## APPENDIX E. GUIDE TO COMPUTER PROGRAM INPUT

This guide is a modification of the one which appeared in Reference [1]. All input to this program is free format. If more than one variable appears on a card, they need only be separated by commas.

An input data deck consists of one J-card, and sets of A-E cards. Each separate groove pattern requires five cards (A, B, C, D, E--in that order).

J Card: Indicates number of grooving patterns in each run

| Variable | Value | Description |
|---|---|---|
| J | Integer | Number of grooving patterns in the run |

A-E Cards: A complete set of A-E cards must be input for each desired groove pattern. Each E card is followed by an A card, except at the end of the grooving pattern. The final E-card is followed by a /* card signaling the end of the program.

A Card: Provides surface roughness information

| Variable | Value | Description |
|---|---|---|
| TD | Real | Depth of macrotexture (in.) |
| ROUGHP | Real | Manning's n value associated with texture depth on the pavement surface |
| ROUGHG | Real | Manning's n value for surface of groove |

B Card: Provides rainfall intensity information

| Variable | Value | Description |
|---|---|---|
| RF | Real | Rainfall intensity (in./hr) |

C Card: Provides slope information

| Variable | Value | Description |
|---|---|---|
| SLOPE | Real | Transverse slope of pavement (ft/ft) |

D Card: Provides groove geometry and spacing parameters (see Figure 3)

| Variable | Value | Description |
|---|---|---|
| ISHAPE | 1 | Indicates rectangular (saw-cut) grooves |
| | 0 | Indicates ungrooved surface |
| GDEPTH | Real | Groove depth (in.). Use 0.00 for ungrooved surface. |
| GWIDTH | Real | Groove top width (in.). Use 0.00 for ungrooved surface. |
| GSPACE | Real | Center-to-center spacing between adjacent grooves (in.). Use WIDTH x 12 for ungrooved surface. |

E Card: Provides pavement size parameters

| Variable | Value | Description |
|---|---|---|
| PLENG | Real | Total distance downslope to be studied (ft) |
| GLENG | Real | Total distance grooves extend downslope (ft). Cannot exceed PLENG. |
| WIDTH | Real | Total width across slope to be studied (ft) |

# APPENDIX F. TYPICAL COMPUTER PROGRAM OUTPUT

FAA RUNWAY DRAINAGE PROGRAM OUTPUT
PENNSYLVANIA STATE UNIVERSITY
PENNSYLVANIA TRANSPORTATION INSTITUTE
NOVEMBER 1982

GROOVED SURFACE

| | |
|---|---|
| TEXTURE DEPTH (INCHES): | 0.0260000 |
| MANNINGS "N" FACTOR(SURFACE): | 0.0500000 |
| MANNINGS "N" FACTOR(GROOVES): | 0.0100000 |
| RAINFALL INTENSITY (IN/HR): | 3.0000000 |
| RUNWAY SLOPE (FT/FT) : | 0.0150000 |
| GROOVE SPACING (IN): | 180.000000 |
| GROOVE DEPTH (IN): | 0.0 |
| GROOVE WIDTH (IN): | 0.0 |
| SURFACE LENGTH (FT) : | 100.000000 |
| GROOVE LENGTH (FT) : | 100.000000 |
| SURFACE WIDTH (FT) : | 15.0000000 |
| TOTAL FLOW AT END OF PLANE(CFS) : | 0.1040384 |
| TOTAL EQUILIBRIUM FLOW TIME (SEC): | 359.350830 |
| GROOVE EQUILIBRIUM LENGTH (FT): | 0.0 |

| SEGMENT | DISTANCE(FT) | WATER DEPTH(IN) | FLOW(CFS/SPACING) | TOTAL FLOW(CFS) | GROOVE FLOW RATIO |
|---|---|---|---|---|---|
| 1 | 1.0000000 | 0.0188946 | 0.0010394 | 0.0010394 | 0.5000000 |
| 2 | 2.0000000 | 0.0286388 | 0.0020791 | 0.0020791 | 0.5000000 |
| 3 | 3.0000000 | 0.0365267 | 0.0031190 | 0.0031190 | 0.5000000 |
| 4 | 4.0000000 | 0.0438083 | 0.0041589 | 0.0041589 | 0.5000000 |
| 5 | 5.0000000 | 0.0496271 | 0.0051988 | 0.0051988 | 0.5000000 |
| 6 | 6.0000000 | 0.0553640 | 0.0062388 | 0.0062388 | 0.5000000 |
| 7 | 7.0000000 | 0.0607290 | 0.0072788 | 0.0072788 | 0.5000000 |
| 8 | 8.0000000 | 0.0657987 | 0.0083189 | 0.0083189 | 0.5000000 |
| 9 | 9.0000000 | 0.0706127 | 0.0093590 | 0.0093590 | 0.5000000 |
| 10 | 10.0000000 | 0.0752206 | 0.0103991 | 0.0103991 | 0.5000000 |
| 15 | 15.0000000 | 0.0959383 | 0.0155998 | 0.0155998 | 0.5000000 |
| 20 | 20.0000000 | 0.1140132 | 0.0208010 | 0.0208010 | 0.5000000 |
| 25 | 25.0000000 | 0.1303471 | 0.0260024 | 0.0260024 | 0.5000000 |
| 30 | 30.0000000 | 0.1454152 | 0.0312040 | 0.0312040 | 0.5000000 |
| 35 | 35.0000000 | 0.1595064 | 0.0364058 | 0.0364058 | 0.5000000 |
| 40 | 40.0000000 | 0.1728118 | 0.0416078 | 0.0416078 | 0.5000000 |
| 45 | 45.0000000 | 0.1854662 | 0.0468099 | 0.0468099 | 0.5000000 |
| 50 | 50.0000000 | 0.1975692 | 0.0520120 | 0.0520120 | 0.5000000 |
| 55 | 55.0000000 | 0.2091967 | 0.0572143 | 0.0572143 | 0.5000000 |
| 60 | 60.0000000 | 0.2204082 | 0.0624166 | 0.0624166 | 0.5000000 |
| 65 | 65.0000000 | 0.2312517 | 0.0676191 | 0.0676191 | 0.5000000 |
| 70 | 70.0000000 | 0.2417665 | 0.0728217 | 0.0728217 | 0.5000000 |
| 75 | 75.0000000 | 0.2519846 | 0.0780243 | 0.0780243 | 0.5000000 |
| 80 | 80.0000000 | 0.2619335 | 0.0832270 | 0.0832270 | 0.5000000 |
| 85 | 85.0000000 | 0.2716367 | 0.0884297 | 0.0884297 | 0.5000000 |
| 90 | 90.0000000 | 0.2811142 | 0.0936326 | 0.0936326 | 0.5000000 |
| 95 | 95.0000000 | 0.2903832 | 0.0988355 | 0.0988355 | 0.5000000 |
| 100 | 100.000000 | 0.2994589 | 0.1040384 | 0.1040384 | 0.5000000 |

RECTANGULAR GROOVES

| | |
|---|---|
| IRREGULAR DEPTH (INCHES): | 0.0260000 |
| MANNINGS "N" FACTOR (SURFACE): | 0.0560000 |
| MANNINGS "N" FACTOR (GROOVES): | 0.0100000 |
| RAINFALL INTENSITY (IN/HR): | 3.0000000 |
| RUNWAY SLOPE (FT/FT) : | 0.0150000 |
| GROOVE SPACING (IN): | 5.0000000 |
| GROOVE DEPTH (IN): | 0.2500000 |
| GROOVE WIDTH (IN): | 0.2500000 |
| SURFACE LENGTH (FT) : | 100.000000 |
| GROOVE LENGTH (FT) : | 100.000000 |
| SURFACE WIDTH (FT) : | 15.0000000 |
| TOTAL FLOW AT END OF PLANE (CFS) : | 0.1040491 |
| TOTAL EQUILIBRIUM FLOW TIME (SEC): | 359.350830 |
| GROOVE EQUILIBRIUM LENGTH (FT): | 9.9470587 |

| SEGMENT | DISTANCE (FT) | WATER DEPTH (IN) | FLOW (CFS/SPACING) | TOTAL FLOW (CFS) | GROOVE FLOW RATIO |
|---|---|---|---|---|---|
| 1 | 1.0000000 | 0.0 | 0.0000289 | 0.0010418 | 0.1005100 |
| 2 | 2.0000000 | 0.0 | 0.0000579 | 0.0020829 | 0.2010232 |
| 3 | 3.0000000 | 0.0 | 0.0000868 | 0.0031244 | 0.3015374 |
| 4 | 4.0000000 | 0.0 | 0.0001157 | 0.0041659 | 0.4020520 |
| 5 | 5.0000000 | 0.0 | 0.0001446 | 0.0052073 | 0.5025667 |
| 6 | 6.0000000 | 0.0 | 0.0001736 | 0.0062488 | 0.6030820 |
| 7 | 7.0000000 | 0.0 | 0.0002025 | 0.0072903 | 0.7035986 |
| 8 | 8.0000000 | 0.0 | 0.0002314 | 0.0083318 | 0.8041188 |
| 9 | 9.0000000 | 0.0 | 0.0002604 | 0.0093734 | 0.9046317 |
| 10 | 10.0000000 | 0.0032405 | 0.0002893 | 0.0104165 | 1.0000000 |
| 15 | 15.0000000 | 0.0499817 | 0.0004338 | 0.0156154 | 1.0000000 |
| 20 | 20.0000000 | 0.0754593 | 0.0005782 | 0.0208156 | 1.0000000 |
| 25 | 25.0000000 | 0.0961413 | 0.0007227 | 0.0260168 | 1.0000000 |
| 30 | 30.0000000 | 0.1181942 | 0.0008672 | 0.0312176 | 1.0000000 |
| 35 | 35.0000000 | 0.1335126 | 0.0010116 | 0.0364190 | 1.0000000 |
| 40 | 40.0000000 | 0.1455692 | 0.0011561 | 0.0416206 | 1.0000000 |
| 45 | 45.0000000 | 0.1596511 | 0.0013006 | 0.0468224 | 1.0000000 |
| 50 | 50.0000000 | 0.1729490 | 0.0014451 | 0.0520243 | 1.0000000 |
| 55 | 55.0000000 | 0.1855971 | 0.0015896 | 0.0572264 | 1.0000000 |
| 60 | 60.0000000 | 0.1976947 | 0.0017341 | 0.0624286 | 1.0000000 |
| 65 | 65.0000000 | 0.2093175 | 0.0018786 | 0.0676309 | 1.0000000 |
| 70 | 70.0000000 | 0.2205288 | 0.0020231 | 0.0728331 | 1.0000000 |
| 75 | 75.0000000 | 0.2313647 | 0.0021677 | 0.0780357 | 1.0000000 |
| 80 | 80.0000000 | 0.2418761 | 0.0023122 | 0.0832383 | 1.0000000 |
| 85 | 85.0000000 | 0.2520912 | 0.0024567 | 0.0884408 | 1.0000000 |
| 90 | 90.0000000 | 0.2620375 | 0.0026012 | 0.0936435 | 1.0000000 |
| 95 | 95.0000000 | 0.2717382 | 0.0027457 | 0.0988463 | 1.0000000 |
| 100 | 100.000000 | 0.2812133 | 0.0028903 | 0.1040491 | 1.0000000 |

RECTANGULAR GROOVES

| | |
|---|---|
| TEXTURE DEPTH (INCHES): | 0.0260000 |
| MANNINGS "N" FACTOR (SURFACE): | 0.0160000 |
| MANNINGS "N" FACTOR (GROOVES): | 0.0100000 |
| RAINFALL INTENSITY (IN/HR): | 3.0000000 |
| RUNWAY SLOPE (FT/FT) : | 0.0150000 |

| | |
|---|---|
| GROOVE SPACING (IN): | 2.5000000 |
| GROOVE DEPTH (IN): | 0.2500000 |
| GROOVE WIDTH (IN): | 0.2500000 |

| | |
|---|---|
| SURFACE LENGTH (FT) : | 100.000000 |
| GROOVE LENGTH (FT) : | 100.000000 |
| SURFACE WIDTH (FT) : | 15.0000000 |

| | |
|---|---|
| TOTAL FLOW AT END OF PLANE (CFS) : | 0.1040601 |
| TOTAL EQUILIBRIUM FLOW TIME (SEC): | 359.350830 |
| GROOVE EQUILIBRIUM LENGTH (FT): | 19.8981040 |

| SEGMENT | DISTANCE (FT) | WATER DEPTH (IN) | FLOW (CFS/SPACING) | TOTAL FLOW (CFS) | GROOVE FLOW RATIO |
|---|---|---|---|---|---|
| 1 | 1.0000000 | 0.0 | 0.0000145 | 0.0010418 | 0.0502550 |
| 2 | 2.0000000 | 0.0 | 0.0000289 | 0.0020829 | 0.1005116 |
| 3 | 3.0000000 | 0.0 | 0.0000434 | 0.0031244 | 0.1507687 |
| 4 | 4.0000000 | 0.0 | 0.0000579 | 0.0041659 | 0.2010260 |
| 5 | 5.0000000 | 0.0 | 0.0000723 | 0.0052073 | 0.2512830 |
| 6 | 6.0000000 | 0.0 | 0.0000868 | 0.0062488 | 0.3015400 |
| 7 | 7.0000000 | 0.0 | 0.0001013 | 0.0072903 | 0.3517992 |
| 8 | 8.0000000 | 0.0 | 0.0001157 | 0.0083318 | 0.4020573 |
| 9 | 9.0000000 | 0.0 | 0.0001302 | 0.0093734 | 0.4523160 |
| 10 | 10.0000000 | 0.0 | 0.0001447 | 0.0104149 | 0.5025743 |
| 15 | 15.0000000 | 0.0 | 0.0002170 | 0.0156224 | 0.7538671 |
| 20 | 20.0000000 | 0.0049121 | 0.0002893 | 0.0208330 | 0.5000000 |
| 25 | 25.0000000 | 0.0502551 | 0.0003616 | 0.0260319 | 0.5000000 |
| 30 | 30.0000000 | 0.0756975 | 0.0004338 | 0.0312322 | 0.5000000 |
| 35 | 35.0000000 | 0.0963431 | 0.0005060 | 0.0364330 | 0.5000000 |
| 40 | 40.0000000 | 0.1143750 | 0.0005783 | 0.0416342 | 0.5000000 |
| 45 | 45.0000000 | 0.1306781 | 0.0006505 | 0.0468356 | 0.5000000 |
| 50 | 50.0000000 | 0.1457230 | 0.0007227 | 0.0520372 | 0.5000000 |
| 55 | 55.0000000 | 0.1597958 | 0.0007950 | 0.0572390 | 0.5000000 |
| 60 | 60.0000000 | 0.1730861 | 0.0008672 | 0.0624410 | 0.5000000 |
| 65 | 65.0000000 | 0.1857280 | 0.0009395 | 0.0676430 | 0.5000000 |
| 70 | 70.0000000 | 0.1978202 | 0.0010117 | 0.0728452 | 0.5000000 |
| 75 | 75.0000000 | 0.2094383 | 0.0010840 | 0.0780475 | 0.5000000 |
| 80 | 80.0000000 | 0.2206816 | 0.0011562 | 0.0832498 | 0.5000000 |
| 85 | 85.0000000 | 0.2316778 | 0.0012285 | 0.0884523 | 0.5000000 |
| 90 | 90.0000000 | 0.2419858 | 0.0013008 | 0.0936549 | 0.5000000 |
| 95 | 95.0000000 | 0.2521980 | 0.0013730 | 0.0988575 | 0.5000000 |
| 100 | 100.000000 | 0.2621614 | 0.0014453 | 0.1040601 | 0.5000000 |

RECTANGULAR GROOVES

| | |
|---|---|
| TEXTURE DEPTH (INCHES): | 0.0260000 |
| MANNINGS "N" FACTOR(SURFACE): | 0.0560000 |
| MANNINGS "N" FACTOR(GROOVES): | 0.0100000 |
| RAINFALL INTENSITY (IN/HR): | 3.0000000 |
| BOUNDARY SLOPE (FT/FT) : | 0.0150000 |

| | |
|---|---|
| GROOVE SPACING (IN): | 1.2500000 |
| GROOVE DEPTH (IN): | 0.2500000 |
| GROOVE WIDTH (IN): | 0.2500000 |

| | |
|---|---|
| SURFACE LENGTH (FT) : | 100.000000 |
| GROOVE LENGTH (FT) : | 100.000000 |
| SURFACE WIDTH (FT) : | 15.0000000 |

| | |
|---|---|
| TOTAL FLOW AT END OF PLANE(CFS) : | 0.1040830 |
| TOTAL EQUILIBRIUM FLOW TIME (SEC) : | 359.350830 |
| GROOVE EQUILIBRIUM LENGTH (FT): | 39.7992385 |

| SEGMENT | DISTANCE(FT) | WATER DEPTH(IN) | FLOW(CFS/SPACING) | TOTAL FLOW(CFS) | GROOVE FLOW RATIO |
|---|---|---|---|---|---|
| 1 | 1.0000000 | 0.0 | 0.0000072 | 0.0010414 | 0.9251275 |
| 2 | 2.0000000 | 0.0 | 0.0000145 | 0.0020829 | 0.0502558 |
| 3 | 3.0000000 | 0.0 | 0.0000217 | 0.0031244 | 0.0753893 |
| 4 | 4.0000000 | 0.0 | 0.0000289 | 0.0041659 | 0.1005129 |
| 5 | 5.0000000 | 0.0 | 0.0000362 | 0.0052073 | 0.1256415 |
| 6 | 6.0000000 | 0.0 | 0.0000434 | 0.0062488 | 0.1507708 |
| 7 | 7.0000000 | 0.0 | 0.0000506 | 0.0072903 | 0.1758996 |
| 8 | 8.0000000 | 0.0 | 0.0000579 | 0.0083318 | 0.2010296 |
| 9 | 9.0000000 | 0.0 | 0.0000651 | 0.0093734 | 0.2261578 |
| 10 | 10.0000000 | 0.0 | 0.0000723 | 0.0104149 | 0.2512870 |
| 15 | 15.0000000 | 0.0 | 0.0001085 | 0.0156224 | 0.3769334 |
| 20 | 20.0000000 | 0.0 | 0.0001447 | 0.0208300 | 0.5025812 |
| 25 | 25.0000000 | 0.0 | 0.0001808 | 0.0260376 | 0.6282294 |
| 30 | 30.0000000 | 0.0 | 0.0002170 | 0.0312453 | 0.7538782 |
| 35 | 35.0000000 | 0.0 | 0.0002531 | 0.0364529 | 0.8795269 |
| 40 | 40.0000000 | 0.0078887 | 0.0002893 | 0.0416661 | 0.5000000 |
| 45 | 45.0000000 | 0.0508777 | 0.0003255 | 0.0469651 | 0.5000000 |
| 50 | 50.0000000 | 0.0761726 | 0.0003616 | 0.0520658 | 0.5000000 |
| 55 | 55.0000000 | 0.0967886 | 0.0003977 | 0.0572662 | 0.5000000 |
| 60 | 60.0000000 | 0.1147363 | 0.0004338 | 0.0624673 | 0.5000000 |
| 65 | 65.0000000 | 0.1310084 | 0.0004699 | 0.0676687 | 0.5000000 |
| 70 | 70.0000000 | 0.1460302 | 0.0005060 | 0.0728703 | 0.5000000 |
| 75 | 75.0000000 | 0.1600849 | 0.0005422 | 0.0780722 | 0.5000000 |
| 80 | 80.0000000 | 0.1733601 | 0.0005783 | 0.0832741 | 0.5000000 |
| 85 | 85.0000000 | 0.1859893 | 0.0006144 | 0.0884762 | 0.5000000 |
| 90 | 90.0000000 | 0.1980708 | 0.0006505 | 0.0936784 | 0.5000000 |
| 95 | 95.0000000 | 0.2096797 | 0.0006867 | 0.0988807 | 0.5000000 |
| 100 | 100.000000 | 0.2208747 | 0.0007228 | 0.1040830 | 0.5000000 |

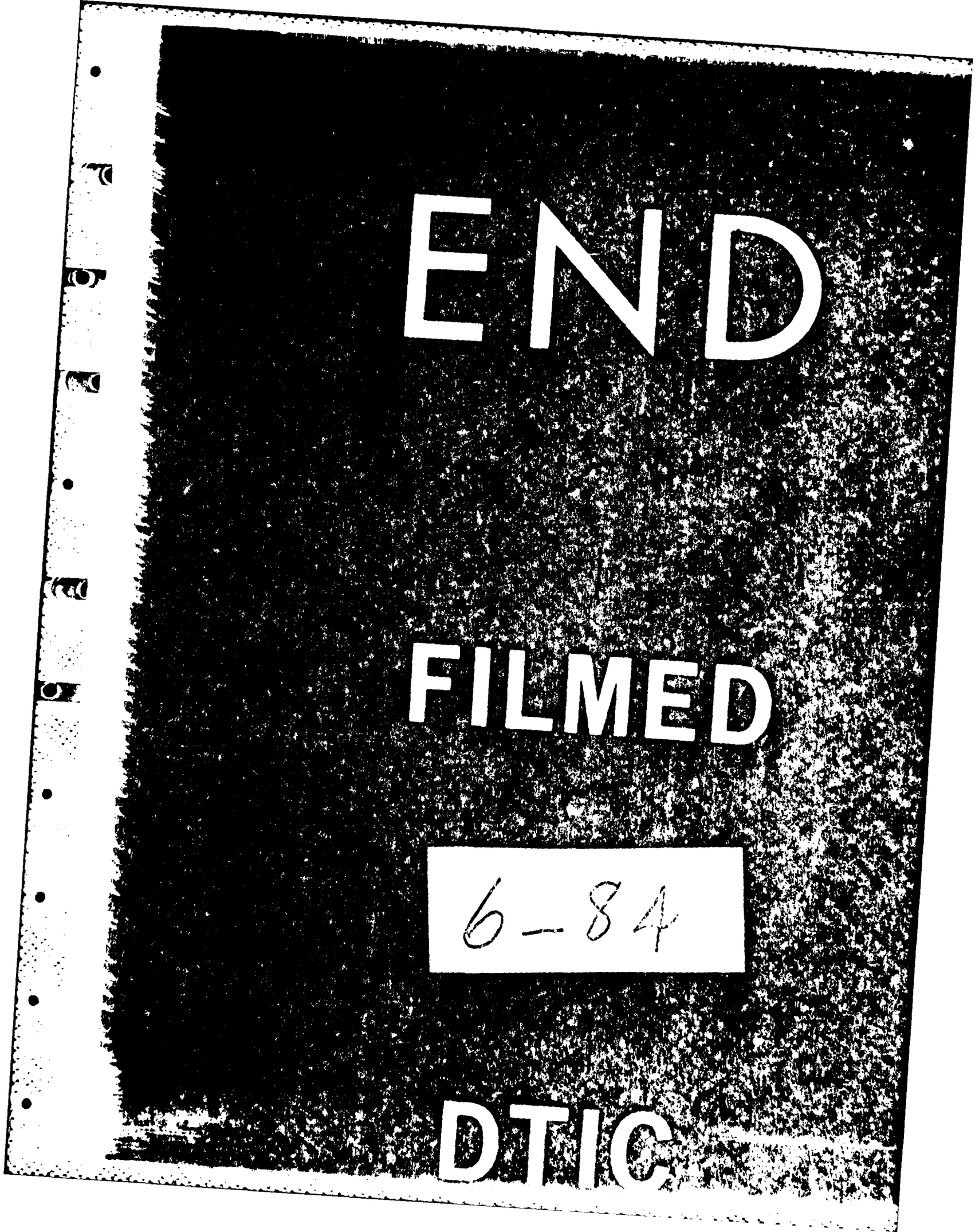
END
FILMED
6-84
DTIC